National School on Neutron and X-Ray Scattering

Oak Ridge and Argonne National Laboratories

Polarized Neutrons

June 3, 2009

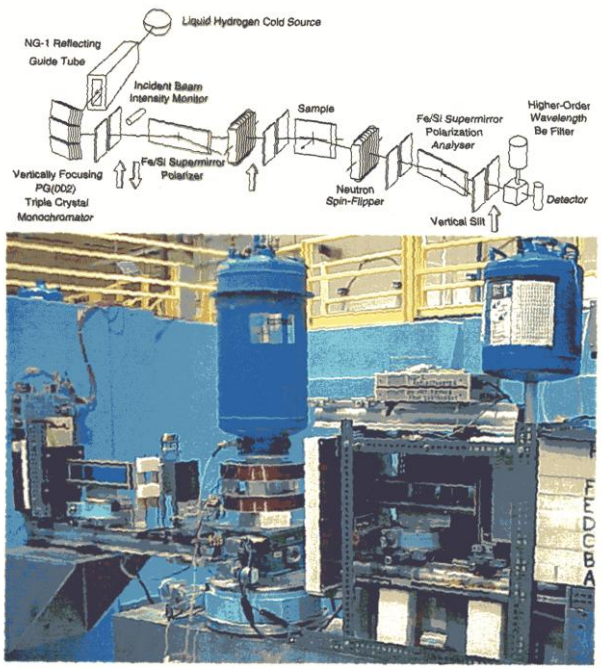

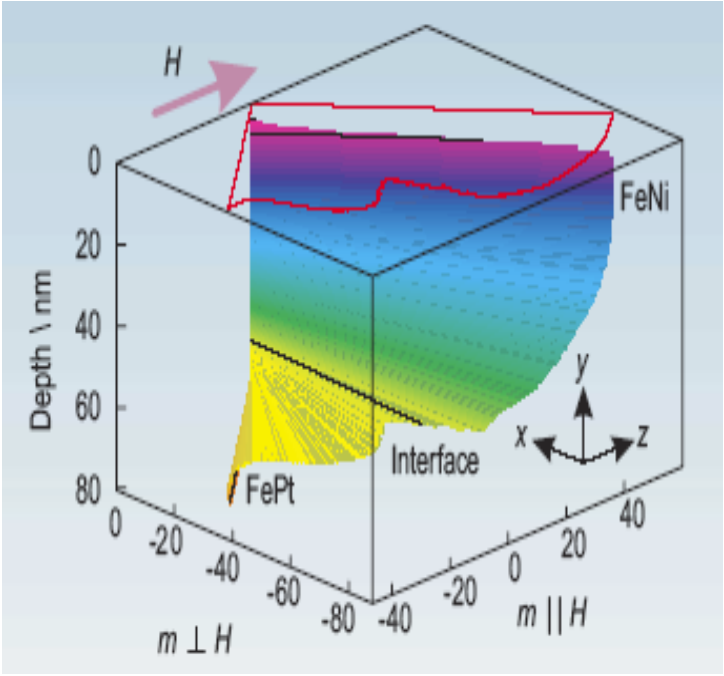

C.F.Majkrzak, *NIST Center for Neutron Research*,
Gaithersburg, MD

G.E. BACON

6

THE PRINCIPLES OF MAGNETIC SCATTERING

6.1. Introduction

AT the beginning of Chapter 2 we explained that, whereas in general the scattering of neutrons by atoms was a nuclear process, nevertheless an exception occurred with magnetic atoms, in the case of which there is additional scattering on account of an interaction between the neutron magnetic moment and the magnetic moment of the atom. We return in this chapter to a discussion of the principles of magnetic scattering and will proceed in the following two chapters to a detailed account of magnetic form-factors and of the way particular types of magnetic structure are revealed.

The determination of the magnetic structures of materials is a task which can achieved only by making measurements of the scattering of neutrons. Indeed it is true to say that our whole conception of the existence of a 'magnetic architecture' within the atomic structure of solids has arisen from observations with neutrons.

The elements of the first transition series which includes iron, cobalt, and nickel, have incomplete 3d shells, as indicated in Table 12 which lists the electronic structures of the free atoms with atomic numbers 19–30. The arrangements of the 3d and 4s shells of some free atoms and ions are shown in Table 13 which also gives the number of unpaired electrons and the spectroscopic ground terms of the ions. These unpaired electrons give rise to a resultant magnetic moment. Interaction of this with the magnetic moment of the neutron, which has a spin quantum number of $\frac{1}{2}$ and a magnetic moment of 1·9 nuclear magnetons, produces neutron scattering which is additional to that produced by the nucleus.

It is worth noting in passing that the fact the neutron, which is an uncharged particle, possesses a magnetic moment is anomalous. A likely explanation is that a neutron spends part of its time dissociated into a proton and a negative π-meson, and although the centres of their respective positive and negative charges do coincide yet the negative charge is more diffuse. This would cause the neutron

POLARIZED NEUTRON REFLECTOMETRY

C.F.Majkrzak (National Institute of Standards and Technology)

Historically, neutron elastic scattering studies have provided a wealth of important atomic scale information about the magnetic structures of condensed matter, a significant part of which could not have been obtained by any other means. In the beginning, magnetic neutron diffraction research was performed primarily on bulk crystals. In more recent years, advances in thin film deposition techniques have made it possible to synthesize a variety of new types of layered magnetic systems, with properties that can be tailored for studies of fundamental scientific interest as well as technological applications. Throughout this still ongoing development, neutron scattering techniques, especially polarized neutron reflectometry (PNR) and diffraction, have made and continue to make significant contributions to the understanding of the physical behavior of magnetic thin films and superlattices (see, for example, the references [1,2]).

Polarized neutron reflectometry can be divided into two broad categories, one of which corresponds to reflection measurements performed with the wavevector transfer Q normal to the film surface, commonly referred to as specular reflectometry, and the other to scattering done with some component of Q lying in the plane of the film. Analysis of the specular polarized neutron reflectivity, measured as a function of Q, yields the in-plane average of the vector magnetization depth profile along the surface normal, with a spatial resolution of less than a nanometer in certain cases. The nonspecular reflectivity, on the other hand, reveals in-plane magnetic structure, such as that associated with domains or artificially patterned surfaces.

In this presentation, we will first show why PNR is such an extraordinarily sensitive, and in some regards unique, probe of magnetic order in thin films and multilayers. We will also illustrate how state-of-the-art methods in experimental and theoretical PNR (see, for example, [3]) can be applied to study current problems in magnetism, including investigations of magnetic semiconductor films and superlattices [4], of particular interest in the relatively new field of "spintronics".

References

1. C.F.Majkrzak, J.Kwo, M.Hong, Y.Yafet, D.Gibbs, C.L.Chien, and J.Bohr, Advances in Physics **40**, 99 (1991).
2. M.R.Fitzsimmons, S.D.Bader, J.A.Borchers, G.P.Felcher, J.K.Furdyna, A.Hoffmann, J.B.Kortright, I.K.Schuller, T.C.Schulthess, S.K.Sinha, M.F.Toney, D.Weller, and S.Wolf, Journal of Magnetism and Magnetic Materials, in press.
3. K.V.O'Donovan, J.A.Borchers, C.F.Majkrzak, O.Hellwig, and E.E.Fullerton, Physical Review Letters **88**, 672011(2002).
4. H.Kepa, G.Springholz, T.M.Giebultowicz, K.I.Goldman, C.F.Majkrzak, P.Kacman, J.Blinkowski, S.Holl, H.Krenn, and G.Bauer, Physical Review B, in press.

HISTORY OF MAGNETIC MATERIALS

BN (BEFORE NEUTRONS)

EMPIRICAL KNOWLEDGE

MACROSCOPIC

NATURAL PERMANENT MAGNETS : MAGNETITE (Fe_3O_4) — SEVERAL THOUSAND YEARS BC

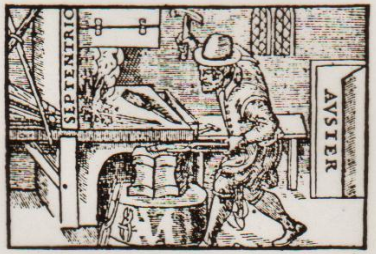

1600 AD GILBERT & MAGNETIZED IRON

DEVELOPMENT OF ALNICO — 1930's

1936 AD DISCOVERY OF NEUTRON (AND m-DIFFR)

AN (ANNO NEUTRONI)

MORE SOPHISTICATED SCIENTIFIC UNDERSTANDING

MICROSCOPIC

CA 1950 AD

STRUCTURE; LONG-RANGE ORDER	DYNAMICS; COLLECTIVE EXCITATIONS	PHASE TRANSITIONS
FERROMAGNETISM ANTIFERROMAGNETISM FERRIMAGNETISM SPIRALS (PLANAR & CONICAL) SPIN DENSITY WAVES CHEMICALLY AMORPHOUS	SPIN WAVES MAGNONS FORCE OR STIFFNESS CONSTANTS	CRITICAL SCATTERING CURIE AND NEEL TEMPERATURES

DOMAINS
WALLS

ELECTRON MOMENT DISTRIBUTION WITHIN UNIT CELL

3D, 2D, & 1D SYSTEMS

NEUTRON SCATTERING

MESOSCOPIC

CA 1980 →

EMPHASIS ON TECHNOLOGICAL APPLICATIONS OF THIN MAGNETIC FILMS : ENGINEERING MAGNETIC PROPERTIES

— INTERLAYER COUPLING & GIANT MAGNETORESISTANCE (GMR) FOR READ HEADS

FUNDAMENTAL SCIENTIFIC INTEREST IN TWO CORRELATION LENGTH SCALES : e.g. Tb

PHYSICAL REVIEW VOLUME 181, NUMBER 2 10 MAY 1969

Polarization Analysis of Thermal-Neutron Scattering*

R. M. MOON, T. RISTE,† AND W. C. KOEHLER
Solid State Division, Oak Ridge National Laboratory, Oak Ridge, Tennessee 37830
(Received 30 December 1968)

A triple-axis neutron spectrometer with polarization-sensitive crystals on both the first and third axes is described. The calculation of polarized-neutron scattering cross sections is presented in a form particularly suited to apply to this instrument. Experimental results on nuclear incoherent scattering, paramagnetic scattering, Bragg scattering, and spin-wave scattering are presented to illustrate the possible applications of neutron-polarization analysis.

I. INTRODUCTION

WE have added a new dimension to measurements of thermal-neutron scattering by constructing, at the Oak Ridge High-Flux Isotope Reactor, a triple-axis spectrometer with polarization-sensitive crystals on both the first and third axes. With this instrument the distribution of scattered neutrons from an initially monochromatic, polarized beam is measured as a [illegible] scattering (++ and −−). The theoretical quantities of greatest interest are the partial cross sections.

This is a different language than is customarily used by theoreticians in describing the scattering of polarized neutrons. The total cross section (summed over final spin states) and the final polarization are calculated as a function of the initial polarization. The polarization equation is a vector relationship giving the magnitude and direction of the final polarization. We measure

Magnetic Neutron Scattering

Neutron: $S = 1/2$; $\mu = 1.91\ \mu_N$

Scattering by atomic magnetic moments: $p = 0.54 \times S \times f(\sin\theta / \lambda) \times 10^{-12}$cm

Magnetic and nuclear scattering amplitudes are of similar magnitude

DIFFRACTION BY MAGNETIC CRYSTALS

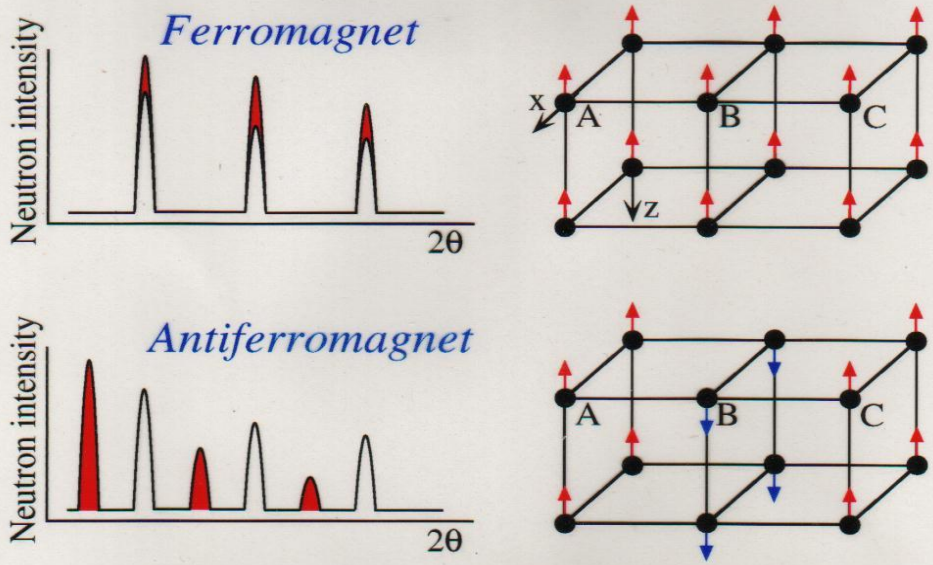

NEUTRON WAVE FUNCTION

$$\Psi = c_+ \begin{pmatrix} 1 \\ 0 \end{pmatrix} e^{i\vec{k}_+ \cdot \vec{r}} + c_- \begin{pmatrix} 0 \\ 1 \end{pmatrix} e^{i\vec{k}_- \cdot \vec{r}}$$

$$k_\pm = n_\pm k_0$$

$$n_\pm^2 = 1 - \frac{2m}{(\hbar k_0)^2}\left(V_N \pm \mu B\right)$$

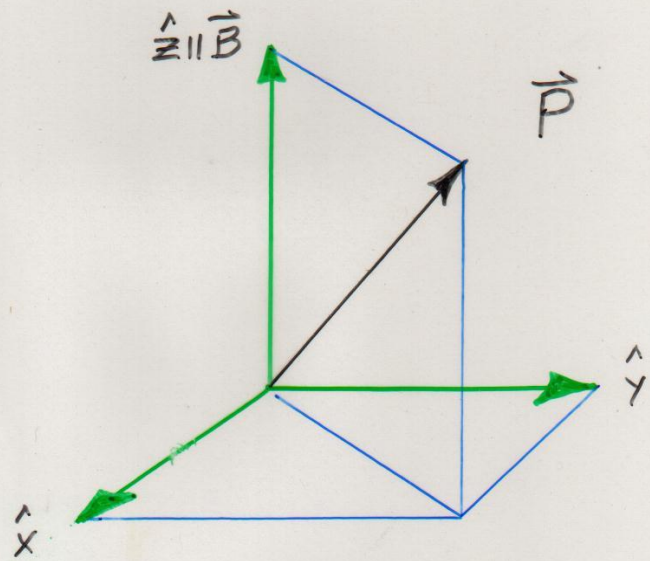

GENERAL MULTILAYER REFLECTIVITY CALCULATION FOR POLARIZED NEUTRONS

$$\left[\frac{-\hbar^2}{2m}\nabla^2 + (V-E)\right]\Psi = 0 \qquad \Psi = \begin{pmatrix}\Psi_+\\ \Psi_-\end{pmatrix}$$

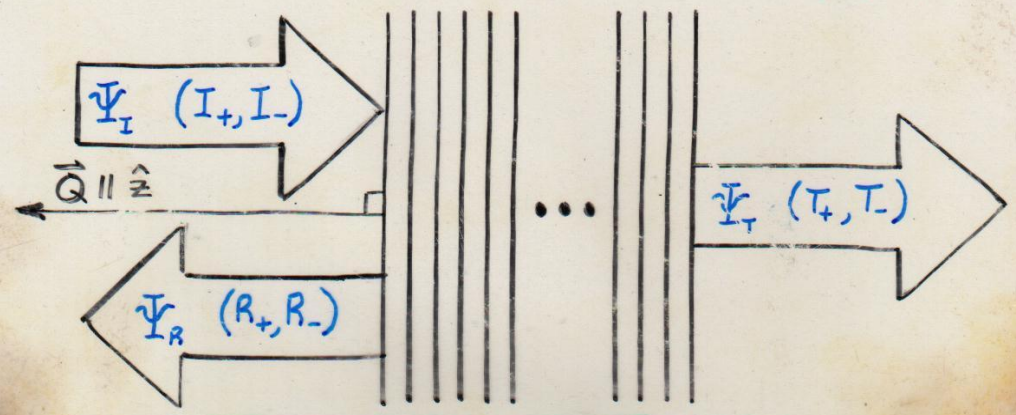

$$V_N = Nb$$

$$V_M = -\vec{\mu}\cdot\vec{B}$$

$$\frac{\partial^2}{\partial z^2}\Psi_+ + \left(\frac{Q^2}{4} - 4\pi\rho_{11}\right)\Psi_+ - 4\pi\rho_{12}\Psi_- = 0$$

$$\frac{\partial^2}{\partial z^2}\Psi_- + \left(\frac{Q^2}{4} - 4\pi\rho_{22}\right)\Psi_- - 4\pi\rho_{21}\Psi_+ = 0$$

$$\underset{(22)}{\rho_{11}} = Nb \underset{(-)}{+} Np\,\sin\theta\sin\phi$$

$$\underset{(21)}{\rho_{12}} = Np\left(\cos\theta \underset{(+)}{-} i\,\sin\theta\cos\phi\right)$$

$$\underline{V_M} = -\underline{\mu} \cdot \vec{B}$$

$$= -\gamma_m \left\{ \underline{S_x} B_x + \underline{S_y} B_y + \underline{S_z} B_z \right\}$$

$$= -\gamma_m \frac{\hbar}{2} \left\{ \begin{pmatrix} 0 & B_x \\ B_x & 0 \end{pmatrix} + \begin{pmatrix} 0 & -iB_y \\ iB_y & 0 \end{pmatrix} + \begin{pmatrix} B_z & 0 \\ 0 & -B_z \end{pmatrix} \right\}$$

$$= -\gamma_m \frac{\hbar}{2} \begin{pmatrix} B_z & B_x - iB_y \\ B_x + iB_y & -B_z \end{pmatrix}$$

$$= \frac{h^2}{2m\pi} \begin{pmatrix} N_{P_z} & N_{P_x} - iN_{P_y} \\ N_{P_x} + iN_{P_y} & -N_{P_z} \end{pmatrix}$$

- ONLY COMPONENTS OF $\vec{B} \perp \vec{Q}$ ARE EFFECTIVE IN SCATTERING NEUTRONS

$$\underline{\mu} = -\gamma_m \frac{\hbar}{2} \left\{ \begin{pmatrix} 0 & 1 \\ 1 & 0 \end{pmatrix} \hat{x} + \begin{pmatrix} 0 & -i \\ i & 0 \end{pmatrix} \hat{y} + \begin{pmatrix} 1 & 0 \\ 0 & -1 \end{pmatrix} \hat{z} \right\}$$

PIECEWISE CONTINUOUS SOLUTION :

$$\begin{pmatrix} T_+ \\ T_- \\ i\frac{Q}{2} T_+ \\ i\frac{Q}{2} T_- \end{pmatrix} = \hat{\mathbb{M}}_{\Pi} \begin{pmatrix} I_+ + R_+ \\ I_- + R_- \\ i\frac{Q}{2}[I_+ - R_+] \\ i\frac{Q}{2}[I_- - R_-] \end{pmatrix}$$

WHERE $|T_+|^2, |T_-|^2$ ARE THE TRANSMISSION PROBABILITIES

AND $|R_+|^2, |R_-|^2$ ARE THE REFLECTION PROBABILITIES

$$\hat{\mathbb{M}}_{\Pi} = \prod_{\ell=L}^{1} \hat{M}_{\ell}$$

($\hat{M}_{\ell}$ IS A 4X4 "TRANSFER" MATRIX CORRESPONDING TO THE ℓ TH LAYER OF A MULTILAYER STRUCTURE)

$$F^{\pm\pm} \propto \sum_{j=1}^{N} \left[b_{s_j} \pm P_{s_j} \cos\phi_j \right] e^{iQu_j}$$

$$F^{\pm\mp} \propto \sum_{j=1}^{N} P_{s_j} \sin\phi_j \, e^{iQu_j}$$

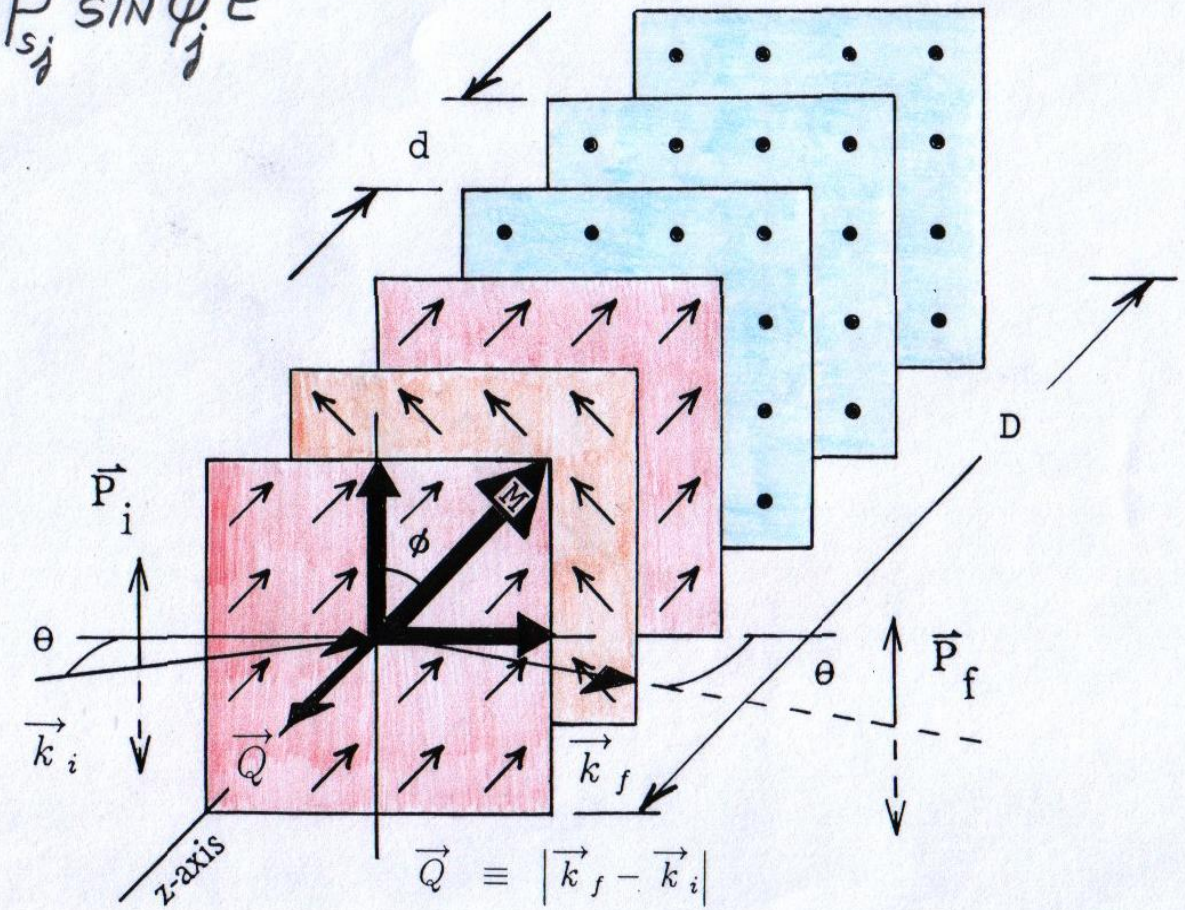

SELECTION RULES FOR SCATTERING OF POLARIZED NEUTRONS BY MAGNETIC MOMENTS

- ONLY MAGNETIZATION COMPONENTS $\perp \vec{Q}$ GIVE RISE TO SCATTERING
- COHERENT NUCLEAR SCATTERING : ALL NSF

- NUCLEAR SPIN INCOHERENT

FIELD AT SAMPLE	SF	NSF
$\vec{H} \parallel \vec{Q}$	2/3	1/3
$\vec{H} \perp \vec{Q}$	"	"

- ANTIFERROMAGNET OR PARAMAGNET

FIELD AT SAMPLE	SF	NSF
$\vec{H} \parallel \vec{Q}$	1	0
$\vec{H} \perp \vec{Q}$	1/2	1/2

- SPIRAL MAGNETIC STRUCTURES WITH SINGLE DOMAIN OF ONE CHIRALITY :

$\vec{H} \parallel \vec{Q}$ $\quad + \rightarrow -$ OR $- \rightarrow +$ SF ONLY,

DEPENDING ON WHETHER SPIRAL IS RIGHT- OR LEFT- HANDED

Polarized Neutron Reflectometry

at the NCNR NG-1 Reflectometer

Scattering experiment determines the correlation of magnetism at two depths separated by $d \sim 2\pi/Q$

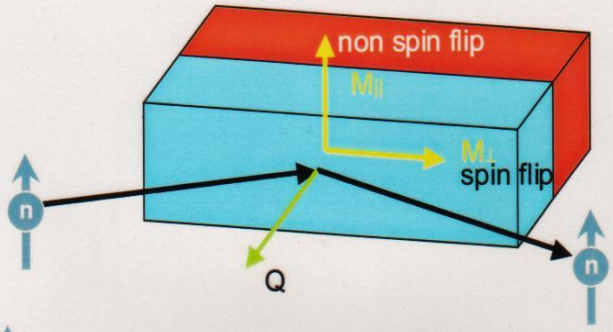

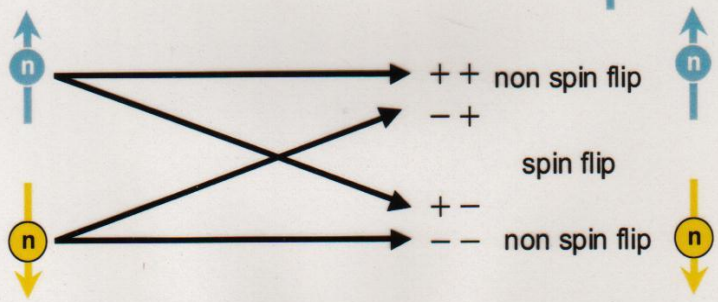

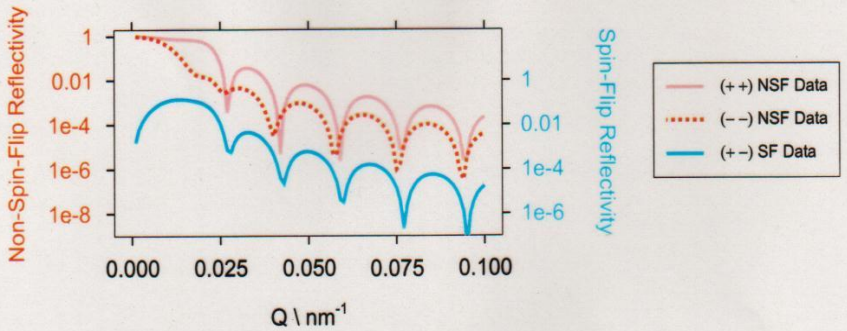

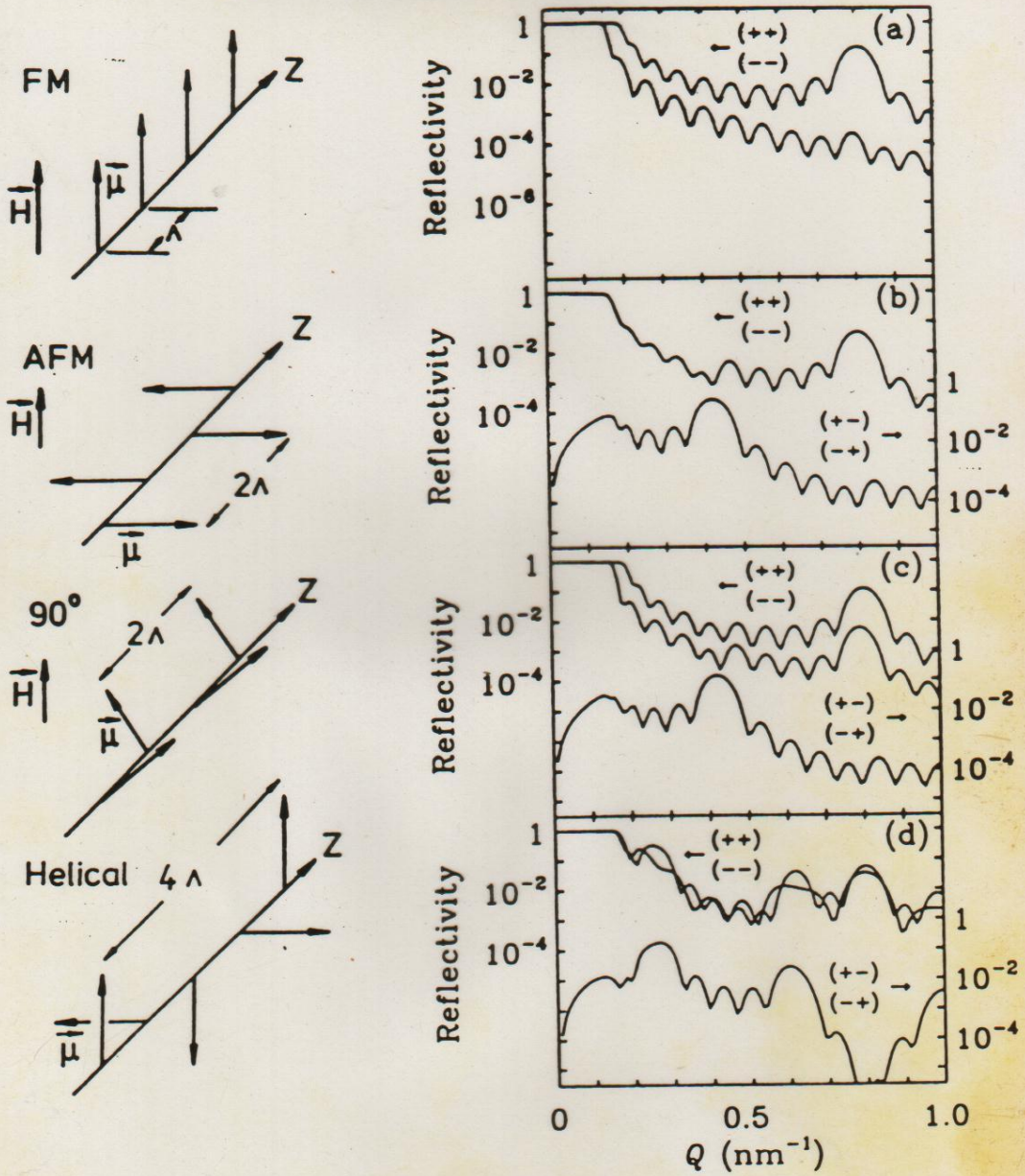

ANKNER, SCHREYER, MAJKRZAK, ZABEL, et al.

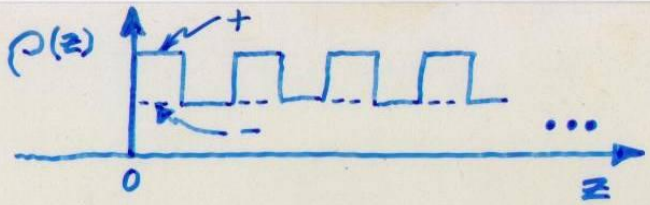

$$|F_\pm|^2 \propto |N_b \pm N_p|^2$$

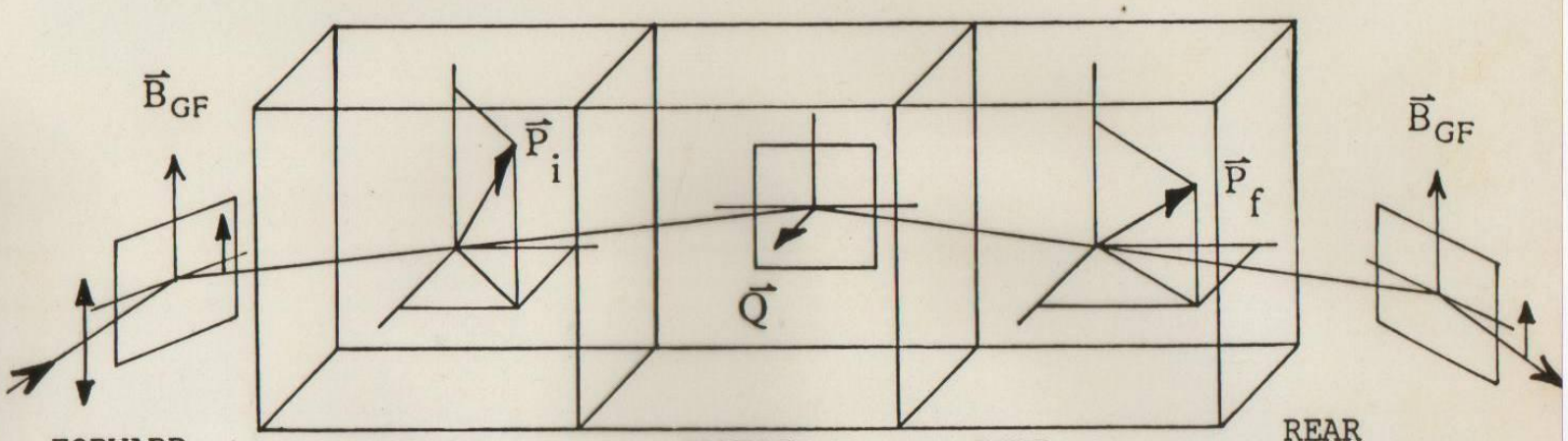

FORWARD POLARIZER

~.95 EFF.

FORWARD FLIPPER OR ROTATION REGION

~.99 EFF.

SAMPLE REGION

REAR FLIPPER OR ROTATION REGION

REAR POLARIZATION ANALYSER

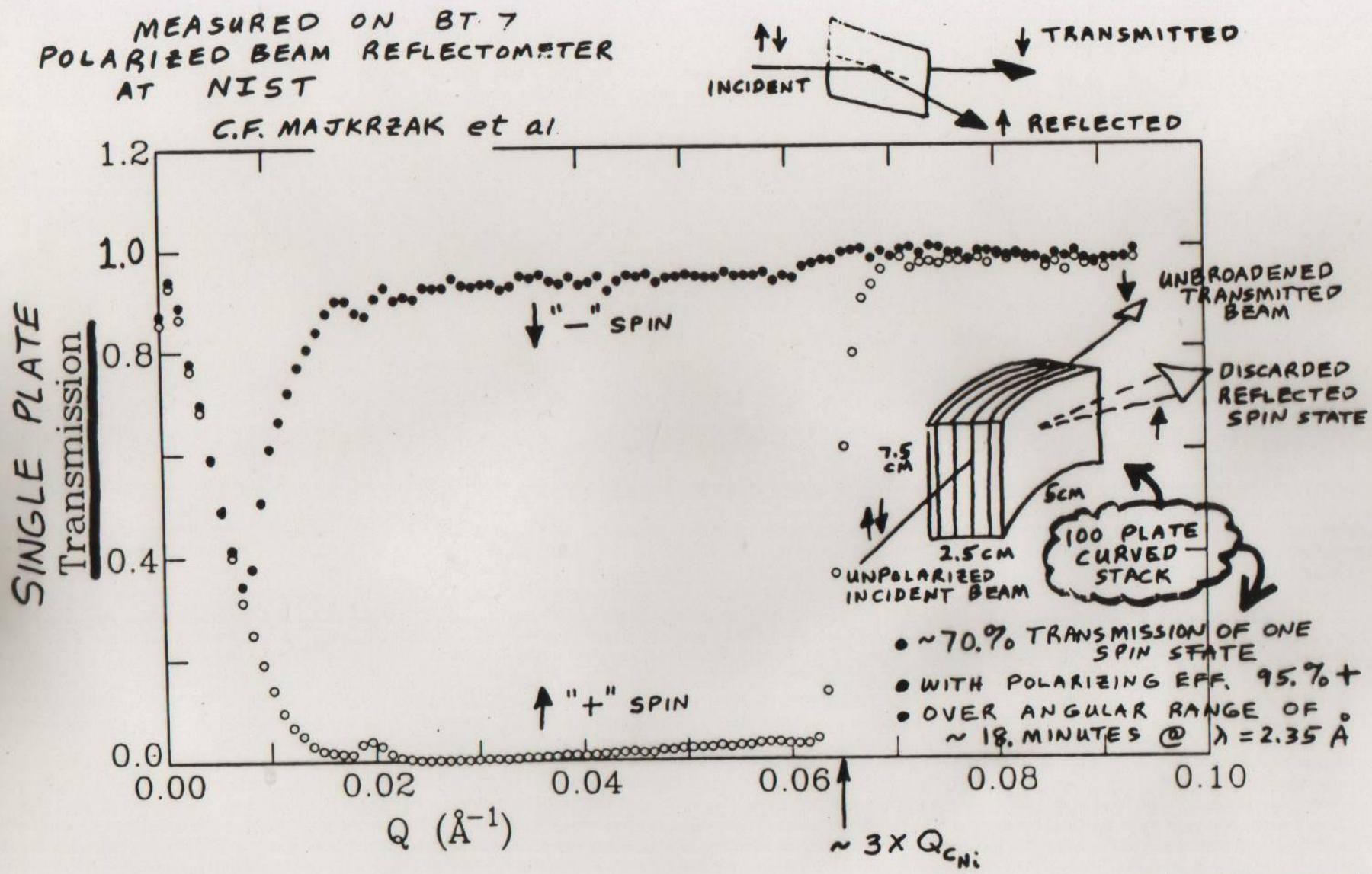

Fe/Si SUPERMIRROR POLARIZER IN TRANSMISSION (SINGLE CRYSTAL Si SUBSTRATE)
(COATING MANUFACTURED BY OSMC COMPANY – J. WOOD)

Figure B

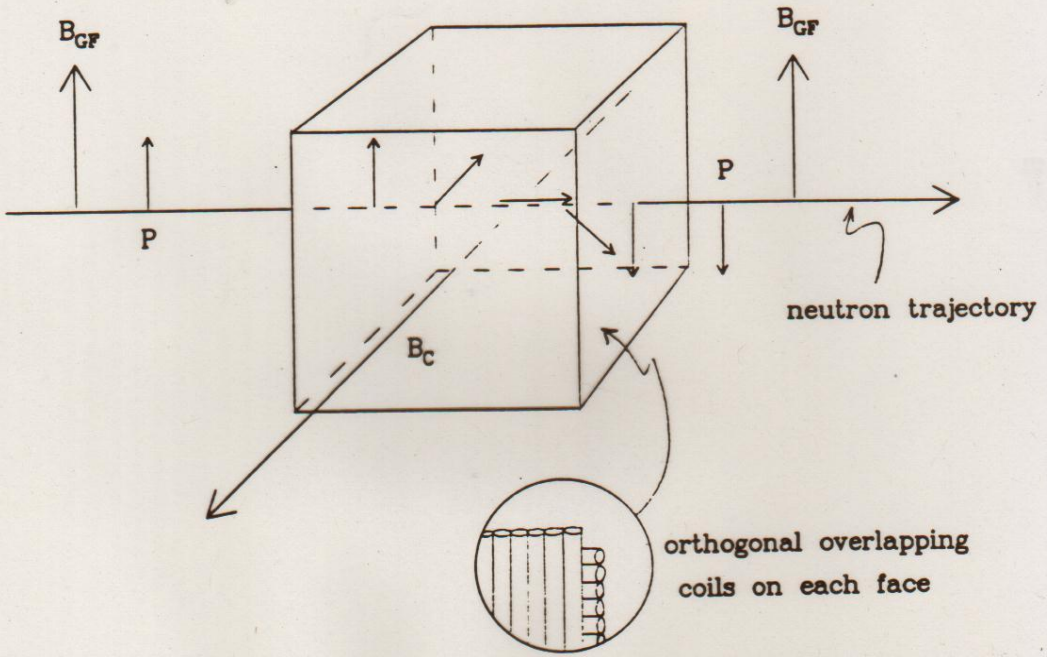

Fig. 5–2

Figure 5-2. Cubic volume defined by three mutually orthogonal, intersecting solenoidal coils of square cross section within which a magnetic field $\vec{B}_c$ is created. Assuming sudden transitions across the coil boundaries, the neutron polarization will precess about the different field direction inside the coil as described in the text. Thus, the neutron polarization $\vec{P}$ can be rotated to any general orientation in space relative to the guide field $\vec{B}_{GF}$.

Polarized Neutron Reflectometry

at the NCNR NG-1 Reflectometer

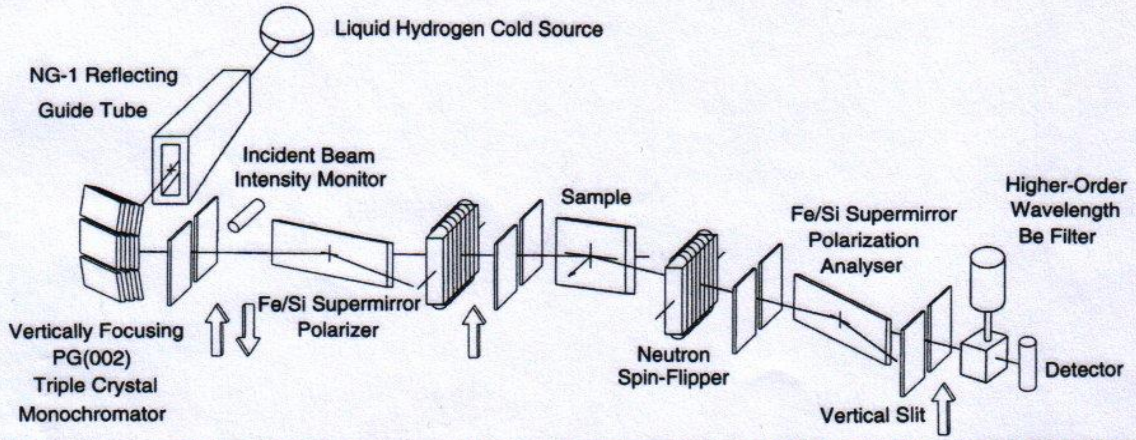

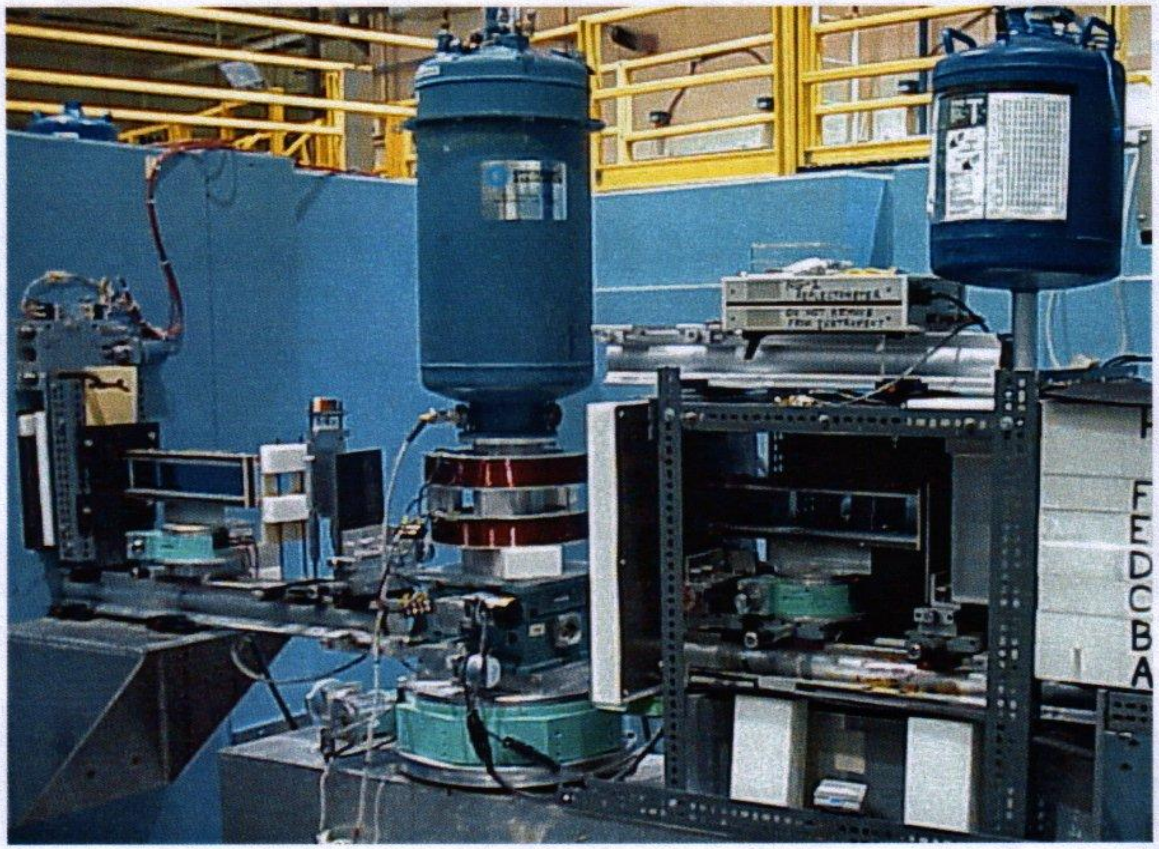

TABLE 2: POLARIZING AND FLIPPING EFFICIENCY CORRECTIONS

$\sigma_{++}, \sigma_{--}, \sigma_{+-}$, and σ_{-+} are defined as the NSF and SF reflectivities, respectively, corresponding to the sample.

$I^{off\ off}$, $I^{on\ on}$, $I^{off\ on}$, and $I^{on\ off}$ are defined as the intenisities measured with front and rear flippers respectively, in "on" (π rotation of the neutron spin) or "off" (no rotation) states.

F, R, f, and r are defined as the front and rear polarizer and front and rear flipper efficiencies, respectively.

The relationship between the intensities measured in the detector and the sample spin-dependent reflectivities are [28]

$$\begin{aligned} I^{off\ off}/\beta = {} & \sigma_{++}(1+F)(1+R) \\ & +\sigma_{-+}(1-F)(1+R) \\ & +\sigma_{--}(1-F)(1-R) \\ & +\sigma_{+-}(1+F)(1-R) \end{aligned}$$

$$\begin{aligned} I^{on\ off}/\beta = {} & \sigma_{++}(1+R)[1+F(1-2f)] \\ & +\sigma_{-+}(1+R)[1-F(1-2f)] \\ & +\sigma_{--}(1-R)[1-F(1-2f)] \\ & +\sigma_{+-}(1-R)[1+F(1-2f)] \end{aligned}$$

$$\begin{aligned} I^{off\ on}/\beta = {} & \sigma_{++}(1+F)[1+R(1-2r)] \\ & +\sigma_{-+}(1-F)[1+R(1-2r)] \\ & +\sigma_{--}(1-F)[1-R(1-2r)] \\ & +\sigma_{+-}(1+F)[1-R(1-2r)] \end{aligned}$$

$$\begin{aligned} I^{on\ on}/\beta = {} & \sigma_{++}[1+F(1-2f)][1+R(1-2r)] \\ & +\sigma_{-+}[1-F(1-2f)][1+R(1-2r)] \\ & +\sigma_{--}[1-F(1-2f)][1-R(1-2r)] \\ & +\sigma_{+-}[1+F(1-2f)][1-R(1-2r)] \end{aligned}$$

The spin-dependent reflectivities can be solved for from the measured intensities if the instrumental polarizing and flipping efficiencies and the constant β are determined.

The constant β is given by

$$2\beta = \frac{I_{NS}^{on\ on} I_{NS}^{off\ off} - I_{NS}^{on\ off} I_{NS}^{off\ on}}{I_{NS}^{on\ on} + I_{NS}^{off\ off} - I_{NS}^{on\ off} - I_{NS}^{off\ on}} \equiv \alpha$$

where the subscript "NS" signifies measurements at zero scattering angle with "no sample" in place. Also,

$$\begin{aligned} I_{NS}^{off\ off}/\alpha &= FR+1 \\ I_{NS}^{on\ off}/\alpha &= FR(1-2f)+1 \\ I_{NS}^{off\ on}/\alpha &= FR(1-2r)+1 \end{aligned}$$

so that f, r, and the product F R can be determined.

If the sample is replaced with a "reference sample" (RS) which has $\sigma_{++} \neq \sigma_{--}$ and $\sigma_{+-} = \sigma_{-+} = 0$ (σ_{++} and σ_{--} need not be known), then F and R can be individually determined.

Fe/Cr SUPERLATTICE : UNCORRECTED REFLECTED INTENSITIES

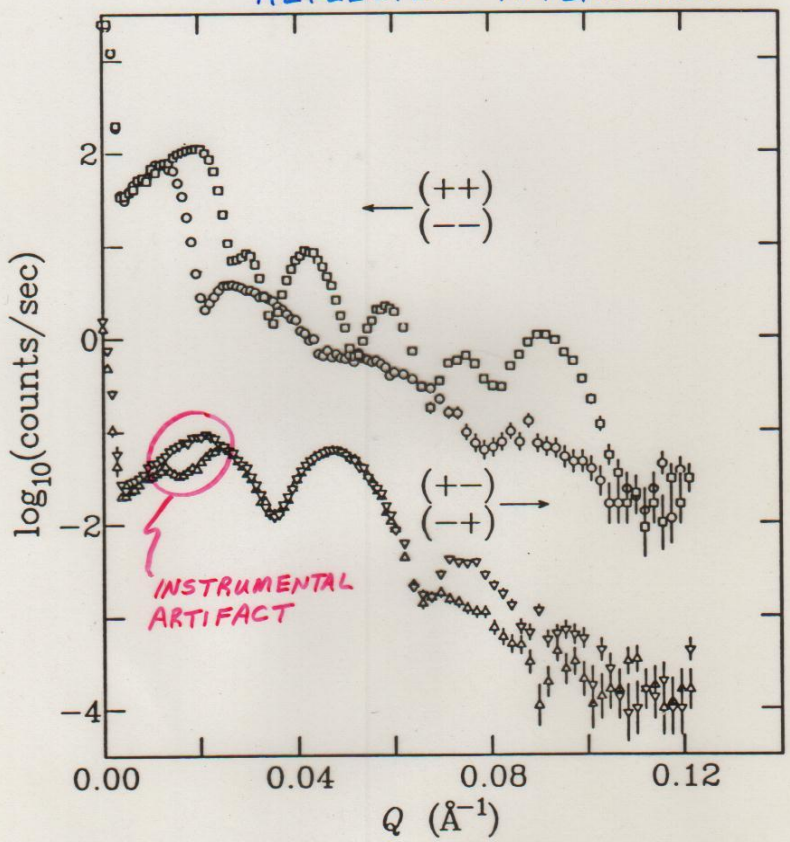

Fe/Cr SUPERLATTICE : REFLECTIVITIES AFTER CORRECTION FOR BEAM FOOTPRINT AND INSTRUMENTAL POLARIZING AND FLIPPING EFFICIENCIES

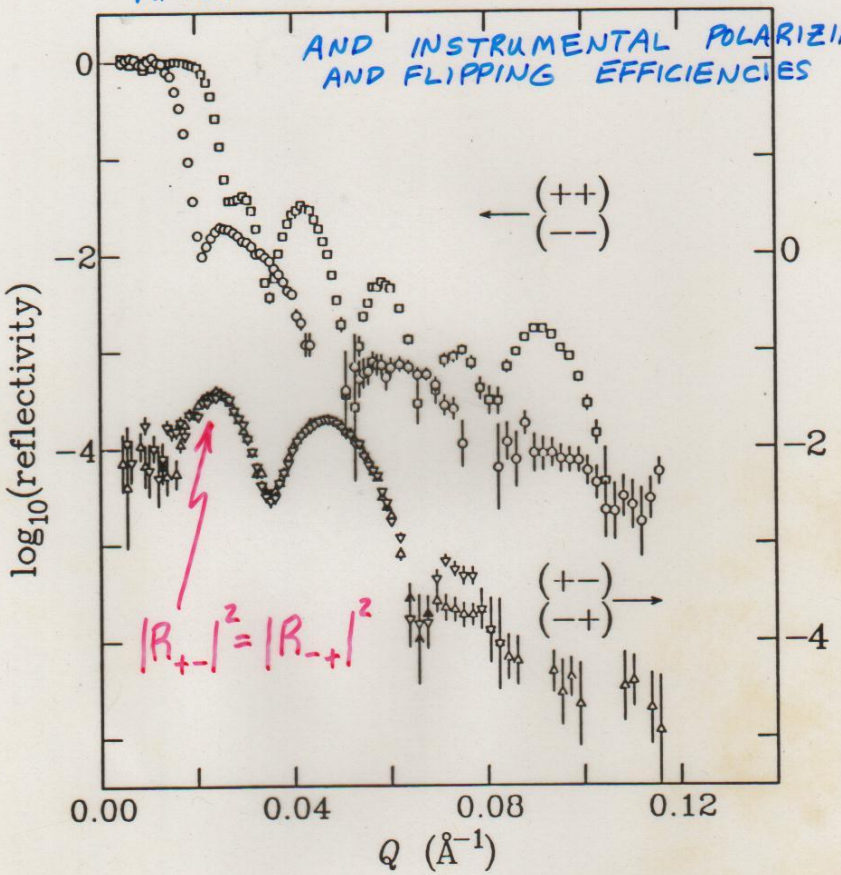

The Nobel Prize in Physics 2007

This year's Nobel Prize in Physics is awarded to ALBERT FERT and PETER GRÜNBERG for their discovery of Giant Magnetoresistance. Applications of this phenomenon have revolutionized techniques for retrieving data from hard disks. The discovery also plays a major role in various magnetic sensors as well as for the development of a new generation of electronics. The use of Giant Magnetoresistance can be regarded as one of the first major applications of nanotechnology.

Better read-out heads for pocket-size devices

Constantly diminishing electronics have become a matter of course in today's IT-world. The yearly addition to the market of ever more powerful and lighter computers is something we have all started to take for granted. In particular, hard disks have shrunk – the bulky box under your desk will soon be history when the same amount of data can just as easily be stored in a slender laptop. And with a music player in the pocket of each and everyone, few still stop to think about how many cds' worth of music its tiny hard disk can actually hold. Recently, the maximum storage capacity of hard disks for home use has soared to a terabyte (a thousand billion bytes).

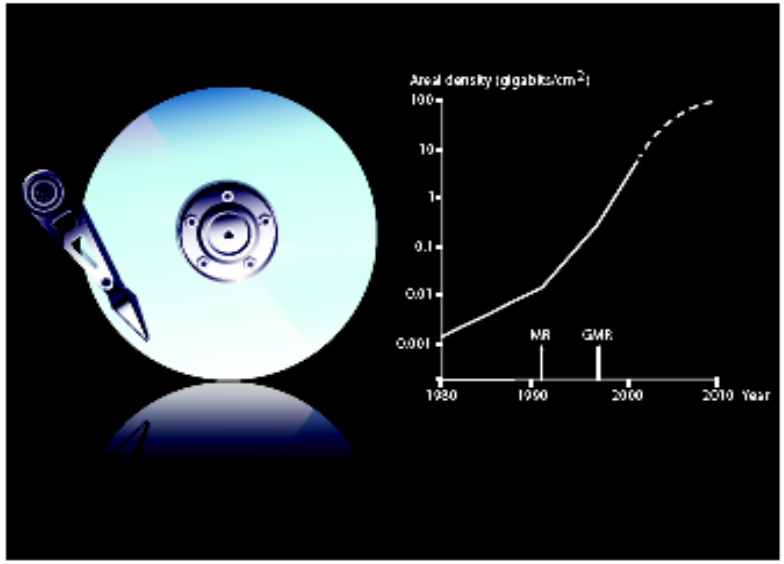

Diagrams showing the accelerating pace of miniaturization might give a false impression of simplicity – as if this development followed a law of nature. In actual fact, the ongoing IT-revolution depends on an intricate interplay between fundamental scientific progress and technical fine tuning. This is just what the Nobel Prize in Physics for the year 2007 is about.

9 October 2007

KUNGL. VETENSKAPSAKADEMIEN
THE ROYAL SWEDISH ACADEMY OF SCIENCES

Scientific Background on the Nobel Prize in Physics 2007

The Discovery of Giant Magnetoresistance

compiled by the Class for Physics of the Royal Swedish Academy of Sciences

The Royal Swedish Academy of Sciences, Information Department, Box 50005, SE-104 05 Stockholm, Sweden
Phone: +46 8 673 95 00, Fax: +46 8 15 56 70, E-mail: info@kva.se, Website: www.kva.se

Nobel Prize® and the Nobel Prize® medal design mark are registered trademarks of the Nobel Foundation

As recounted in the “Scientific Background” material referred to on the left side of the page, prior to the discovery of the GMR effect by Gruenberg, polarized neutron diffraction studies of magnetic superlattices revealed an unambiguous coupling between magnetic layers across intervening nonmagnetic spacers. The interlayer coupling (IEC) observed in this neutron diffraction work was explained in terms of long-range exchange interactions, for example, the RKKY (Ruderman Kittel Kasuya Yosida) interaction. Interestingly, the underlying mechanism responsible for GMR was thus known about before the effect itself was discovered! Much of the original neutron diffraction work was performed at the NIST (then NBS) neutron scattering facility by scientists including James Rhyne, Ross Erwin, and Julie Borchers, some of whom continue related forefront research today at the NCNR.
This is an example of the continuing importance of neutron scatttering as a fundamental probe of condensed matter.

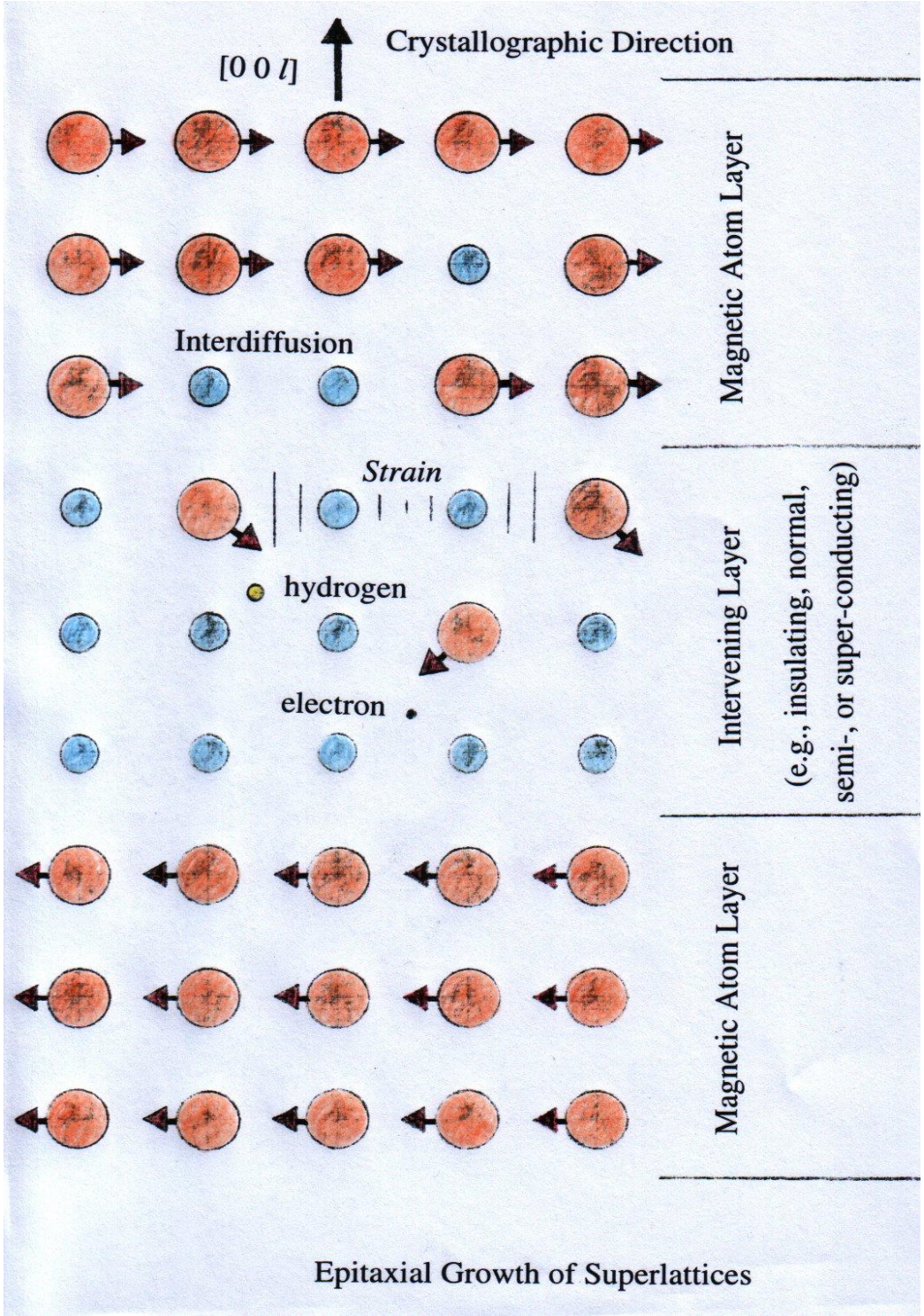

Epitaxial Growth of Superlattices

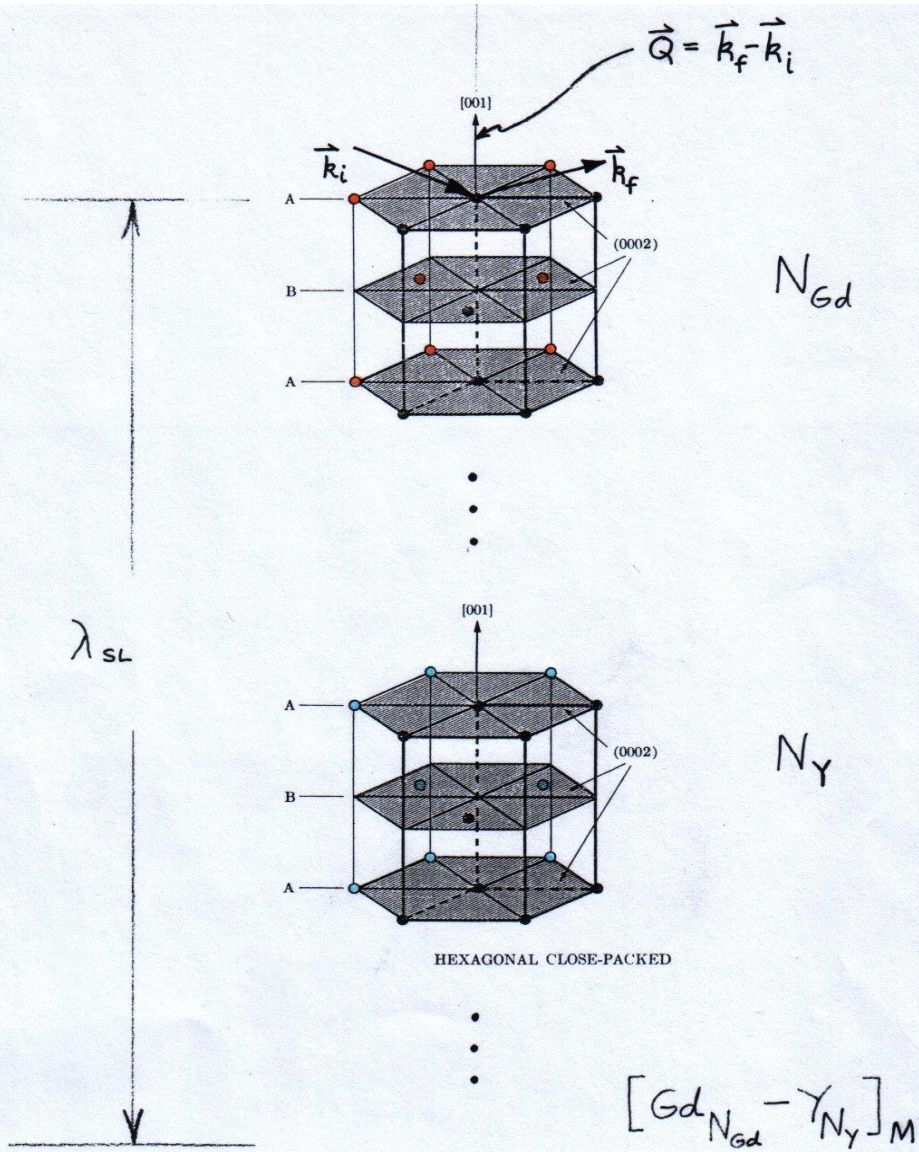

Y(002) SEED LAYER
Nb (110) BUFFER LAYER
Al_2O_3 $(11\bar{2}0)$ SUBSTRATE

ATE011 92

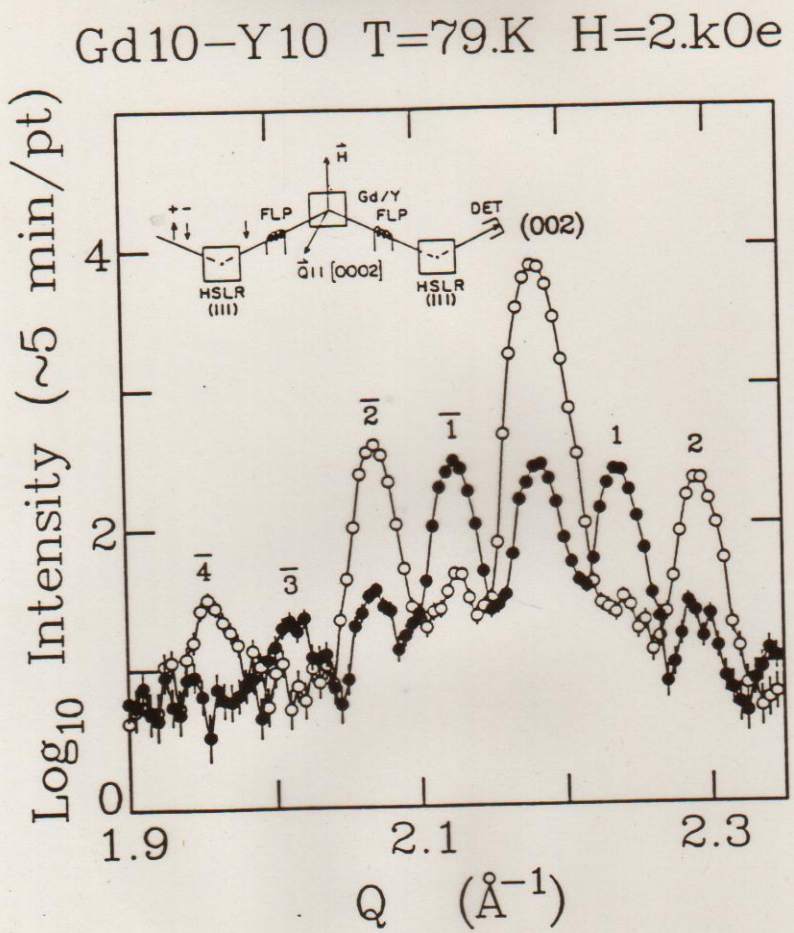

Fig. 7−1

Figure 7-1. NSF (open circles) and SF (filled circles) scattering from a [Gd_{10} - Y_{10}] superlattice as described in the text. The data have not been corrected for instrumental polarizing and flipping efficiencies (the SF scattering at the (002) position is predominantly, if not entirely, instrumental in origin). The SF scattering which appears at values of Q corresponding to a doubling of the chemical bilayer spacing (odd-numbered satellites) is consistent with an antiferromagnetic alignment (for an applied field approaching zero) of neighboring ferromagnetic Gd layers as depicted schematically in Figure 7-2. (After Majkrzak et al. (1986)).

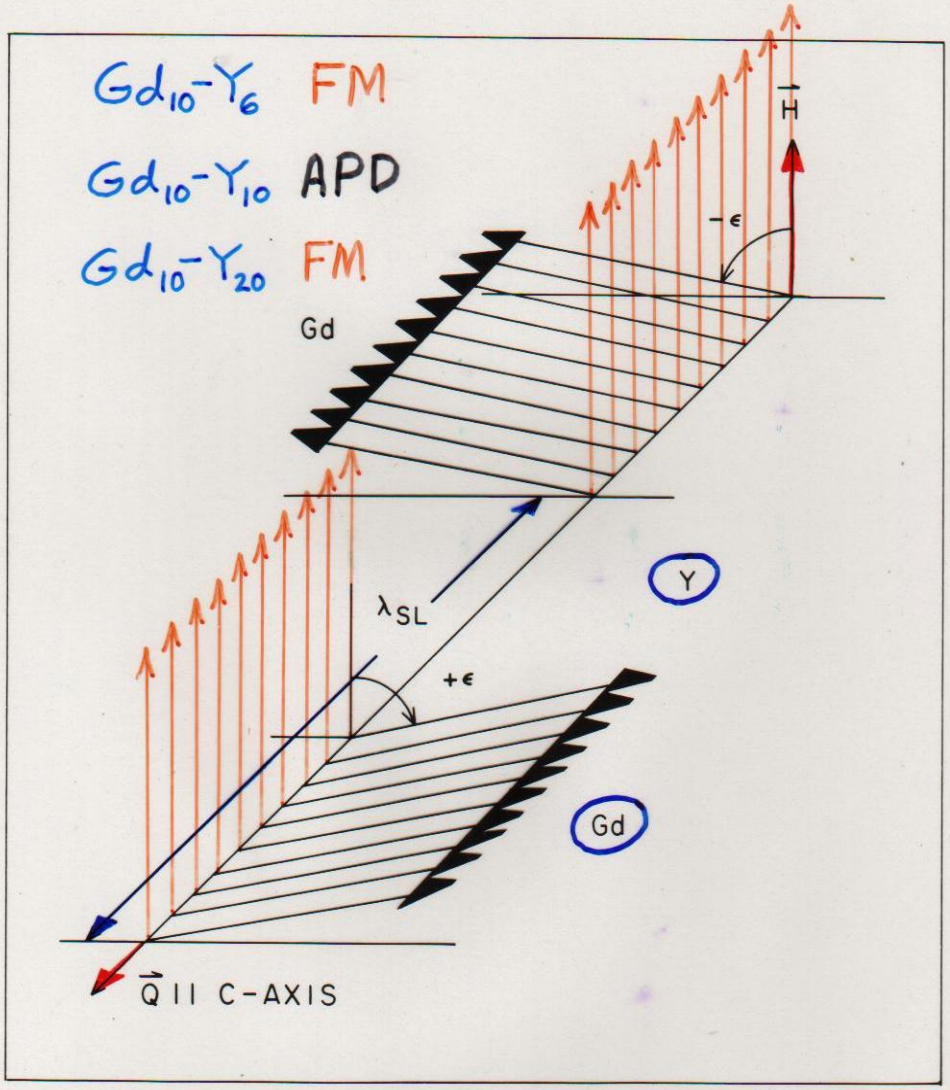
Gd_{10}-Y_6 FM
Gd_{10}-Y_{10} APD
Gd_{10}-Y_{20} FM
Gd
$\vec{H}$
$-\epsilon$
λ_{SL}
$+\epsilon$
Y
Gd
$\vec{Q}$ II C-AXIS

• m-diffr. meas.

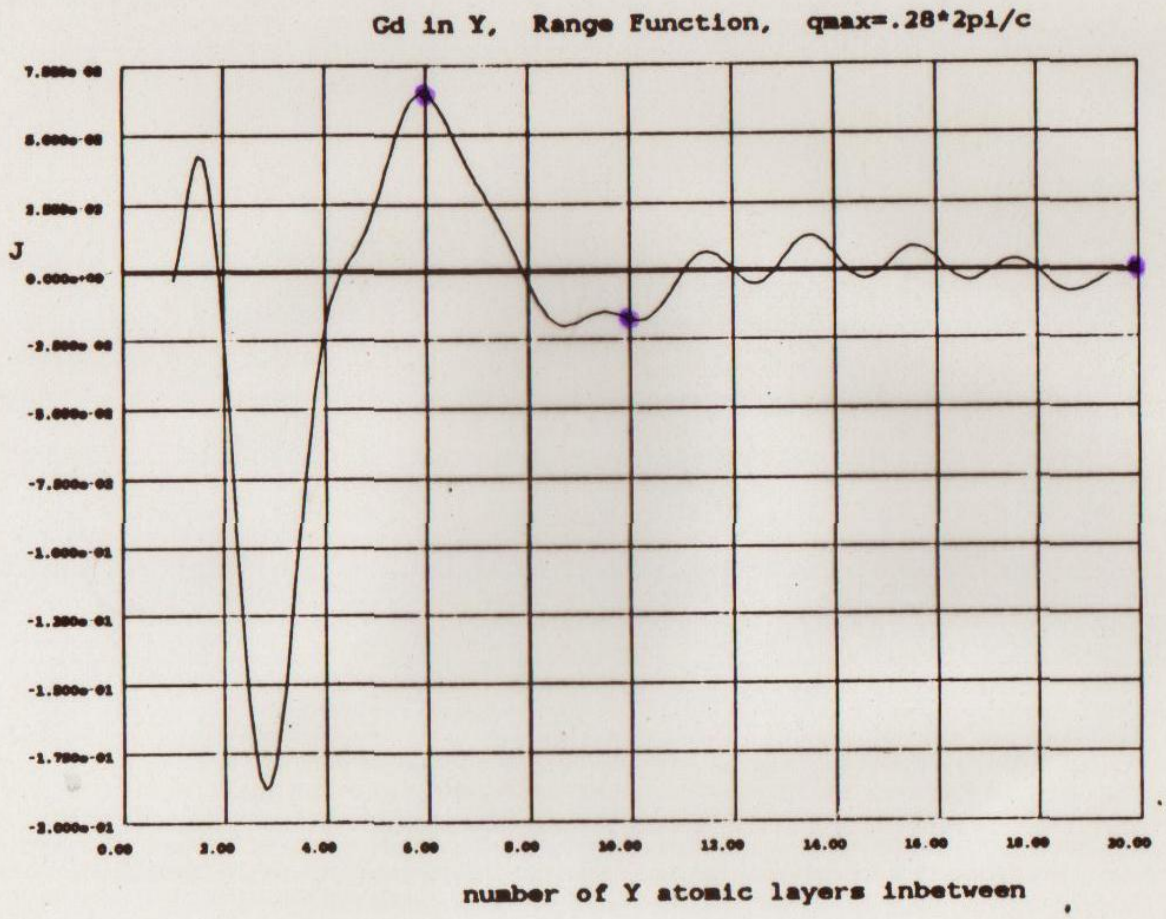
Gd in Y, Range Function, qmax=.28*2pi/c
J
0.00
2.00
4.00
6.00
8.00
10.00
12.00
14.00
16.00
18.00
20.00
number of Y atomic layers inbetween

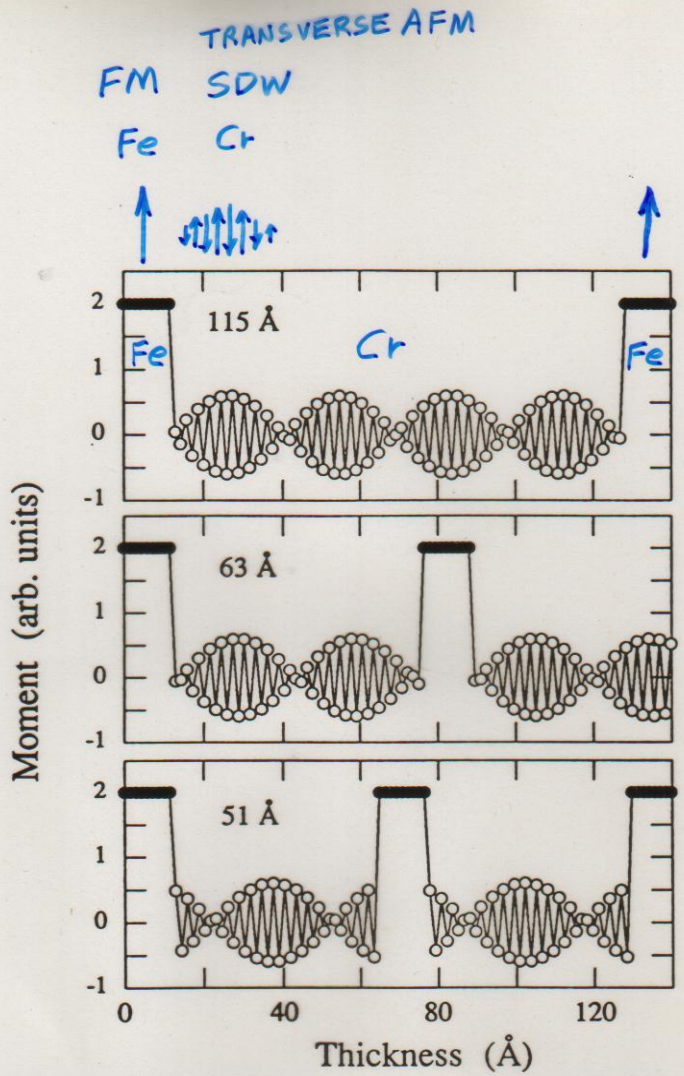

Fe/Cr SUPERLATTICES (GMR)

FULLERTON, BADER, & ROBERTSON

Figure 3

SCHREYER, ZEIDLER, ZABEL, ANKNER, MAJKRZAK, SCHÄFER, & GRÜNBERG, THIS CONFERENCE

NONCOLLINEAR Fe/Cr (001)

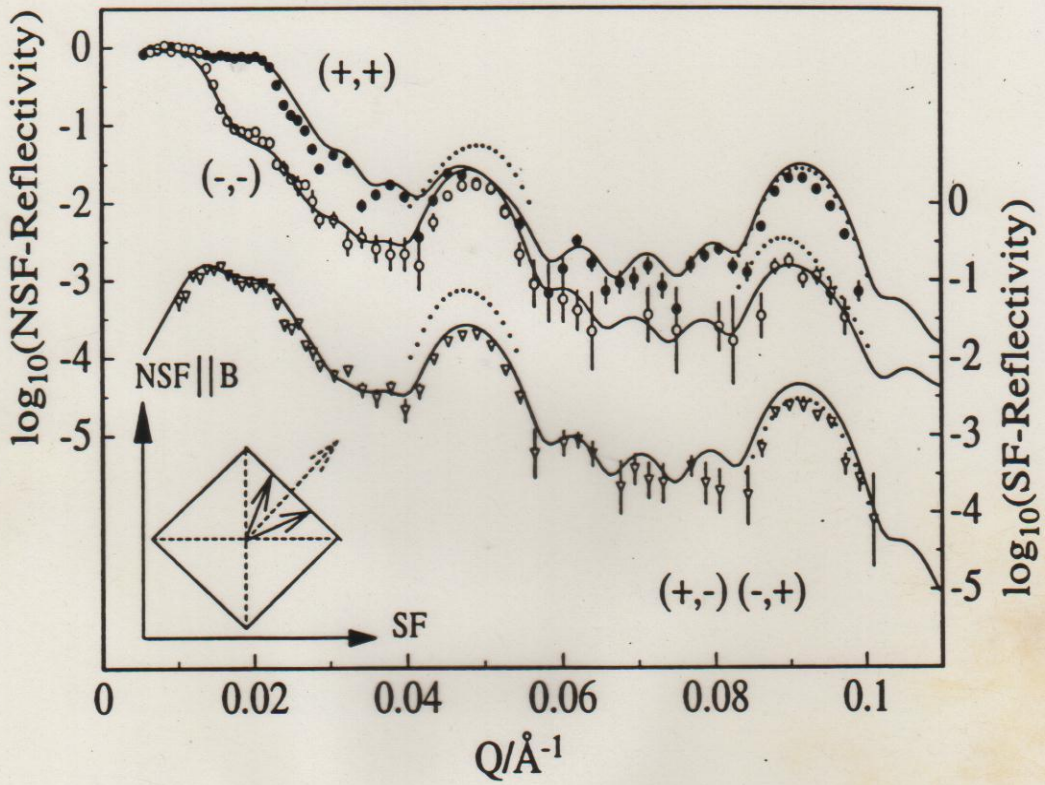

····· 90° ∡

—— 50° ∡

$$E = \underbrace{-J_1 \frac{\vec{M}_1 \cdot \vec{M}_2}{|\vec{M}_1||\vec{M}_2|}}_{\text{BILINEAR}} \underbrace{- J_2 \left(\frac{\vec{M}_1 \cdot \vec{M}_2}{|\vec{M}_1||\vec{M}_2|} \right)^2}_{\text{BIQUADRATIC}}$$

EXCHANGE COUPLING

A. Schreyer et al.

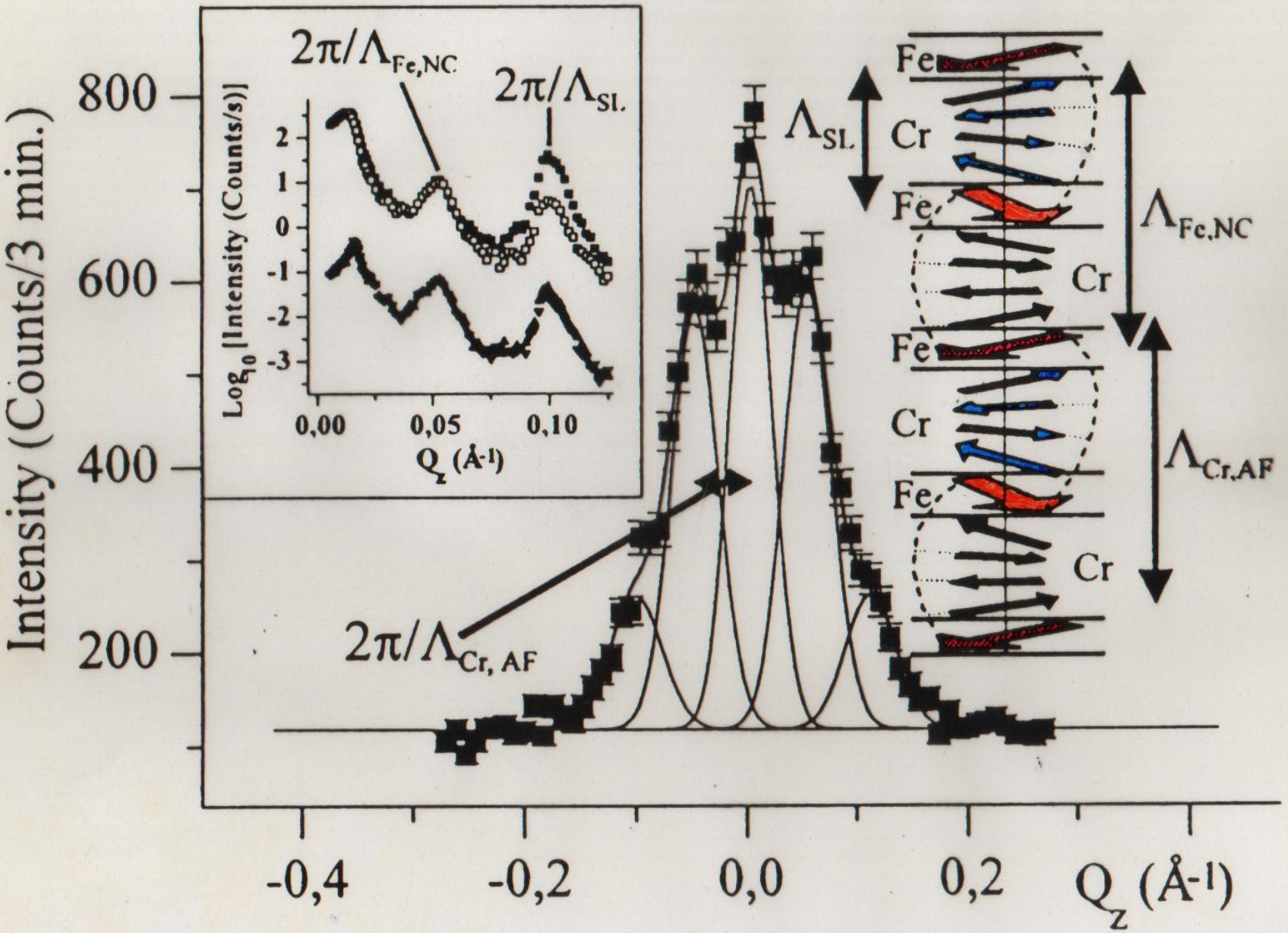

Pinpointing Chiral Structures with Front/Back Polarized Neutron Reflectometry

K. V. O'Donovan, J. A. Borchers, and C. F. Majkrzak
NIST Center for Neutron Research
National Institute of Standards and Technology
Gaithersburg, MD 20899-8562

O. Hellwig, E. E. Fullerton
IBM Almaden Research Facility
San Jose, CA 95120-6001

We have developed a new method of using polarized neutron reflectometry (PNR) to extract the structure of buried magnetic spirals in magnetic films. This technique improves upon earlier methods by being particularly sensitive to the presence of magnetic twists vis-à-vis structures in which the magnetization direction does not vary appreciably. Tracking the formation and growth of twists may solve a number of puzzles that hamper the development of magnetic thin film devices.

In collaboration with IBM scientists, we have applied the technique to a thin-film exchange-spring magnet and confirmed that the results may violate the current theory regarding the behavior of such magnets. It has been predicted that exchange-spring magnets, comprised of soft and hard ferromagnets in close proximity, are a composite that has a strong moment and does not readily demagnetize [1]. Therefore, exchange-spring magnets should give industry the ability to make much smaller permanent magnets for use in the magnetic recording devices, and elsewhere. As a side effect, when a small external magnetic field is opposed to that of the magnet, the portion of the soft ferromagnet farthest from the hard ferromagnet may twist into alignment with the field. When the field is removed, the soft ferromagnet untwists. The film provided by IBM consists of the hard ferromagnet $Fe_{55}Pt_{45}$ topped by the soft ferromagnet $Ni_{80}Fe_{20}$ [2].

Figure 1 shows a simplified diagram of the behavior predicted by current theories [1]. A magnetic field of 0.890 T, provided by an electromagnet, is sufficient to align both the soft and the hard layers of our exchange-spring magnet, as shown on the left. When a modest reverse field (on the order of 0.025 T) is applied to the exchange spring magnet, only the top of the soft layer will realign with the magnetic field. The hard layer remains pinned in the original direction, and a continuous twist is induced in the soft layer, as the direction of magnetization changes smoothly between the reverse field direction to the aligning field direction.

Although there are many alternatives to PNR to measure the magnetization, typically they measure only the average orientation of the magnetic spins, and cannot readily distinguish a spiral from a structure in which all the spins are canted with respect to an external field. PNR can extract the depth-dependence of the magnetic and chemical structure. We have studied the sample over a wide range of external magnetic fields, and can track the development of the spiral with field [3].

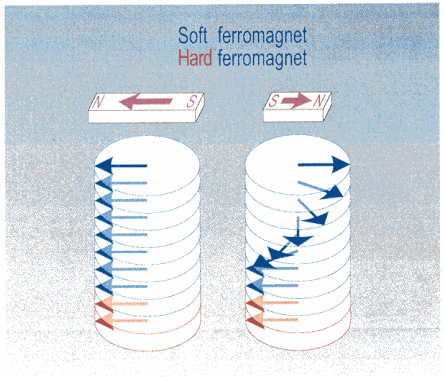

FIGURE 1. Model for field behavior of exchange-spring magnets. On the left the magnet has been aligned by a large external magnetic field. On the right a smaller field opposed to the first field causes a twist to form in the soft ferromagnet, while the hard ferromagnet remains aligned.

A PNR experiment begins with neutrons whose magnetic moments are aligned parallel (+) or opposite (–) to the external magnetic field. When the magnetization of the sample is perpendicular to this magnetic field, the neutron moment precesses as it interacts with the sample. When this happens the spin-flip (SF) reflectivities R^{+-} and R^{-+} are strong. If the magnetization of the sample is parallel to the external magnetic field, no precession occurs, but the non-spin-flip (NSF) reflectivities R^{++} and R^{--} will differ. The NSF reflectivities also provide information about the chemical structure of the film.

Our new modification of the PNR method greatly enhances the contrast between colinear and certain non-colinear magnetic structures [4]. We first measure the reflectivity with neutrons glancing off the front surface of the material, and then repeat with neutrons glancing off the back surface. The experiment is akin to holding the plane of the film up to a "magnetic mirror" to see whether the mirror image is the same as the original structure. In a colinear structure, all the spins are aligned along a common direction, and the mirror image is very much like the original structure.

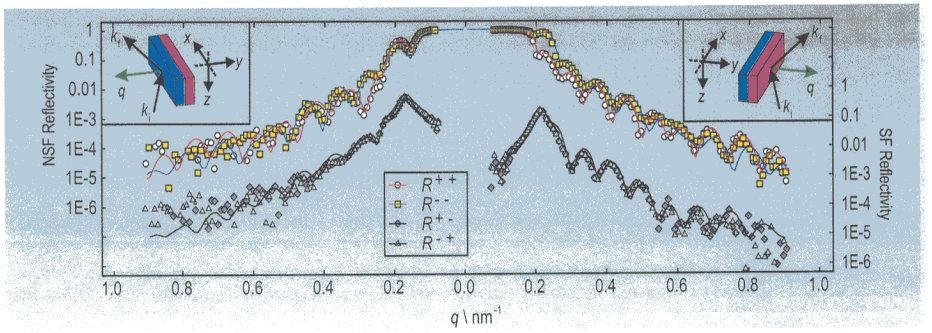

FIGURE 2. Reflectivity of a $Ni_{80}Fe_{20}|Fe_{55}Pt_{45}$ bilayer. The front reflectivity is plotted on the right while the back reflectivity is plotted on the left. The SF reflectivities R^{+-} and R^{-+} are plotted against the right ordinate axis. The NSF reflectivities R^{++} and R^{--} are plotted against the left ordinate axis.

But the mirror image of a magnetic twist to the right is a magnetic twist to the left. Therefore, if the front and back reflectivities are significantly different, we can deduce the presence of a spiral. Fitting the data confirms the spiral's existence.

Figure 2 shows data collected at 0.026 T after aligning in -0.89 T. Fits to the data are shown as solid lines. The data from the front reflectivity are shown on the right, and the data from the back reflectivity are shown on the left. The spin-flip (SF) reflectivities R^{+-} and R^{-+} are plotted against the right-hand axis, which have been shifted relative to the NSF reflectivities R^{++} and R^{--} plotted against the left axis. At $q = 0.2$ nm^{-1}, there is a splitting in the front NSF reflectivity that is much more pronounced than that of the back reflectivity at the same q. This is a hallmark of the spiral structure.

Figure 3 shows the magnetic structure that gives the excellent fit to the data plotted in Fig. 2. The location of the hard/soft interface is marked in Fig. 3. Surprisingly, we discover the spiral invades the hard ferromagnet even at extremely low fields. Current theory predicts that when this occurs, the soft ferromagnet will not be able to untwist fully. Yet, other magnetic studies show that our exchange-spring magnet does untwist when this field is removed. Thus, our PNR measurements have identified a shortcoming of current theory.

With this new technique, NIST is now able to better characterize the magnetic properties of thin films, which can improve the capability and reliability of industrial devices for magnetic recording and sensing.

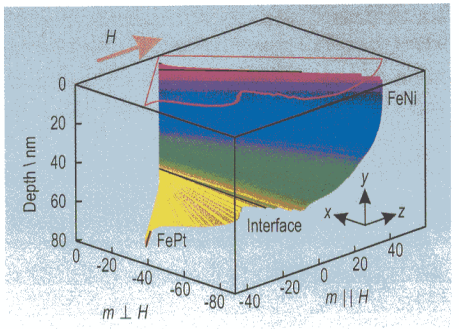

FIGURE 3. Fitted magnetization of the data presented in Fig. 2. The front of the sample is at a depth of 0 nm and the back is at a depth of 70 nm. The red curve is a projection of the magnetic structure into the plane of the front surface.

References

[1] E. F. Kneller and R. Hawig, IEEE Trans. Magn. **27**, 3588 (1991).

[2] O. Hellwig, J. B. Kortright, K. Takano, and E. E. Fullerton, Phys. Rev. **B62**, 11694 (2000).

[3] K. V. O'Donovan, *et al.*, in preparation.

[4] K. V. O'Donovan, *et al.*, submitted to Applied Physics A.

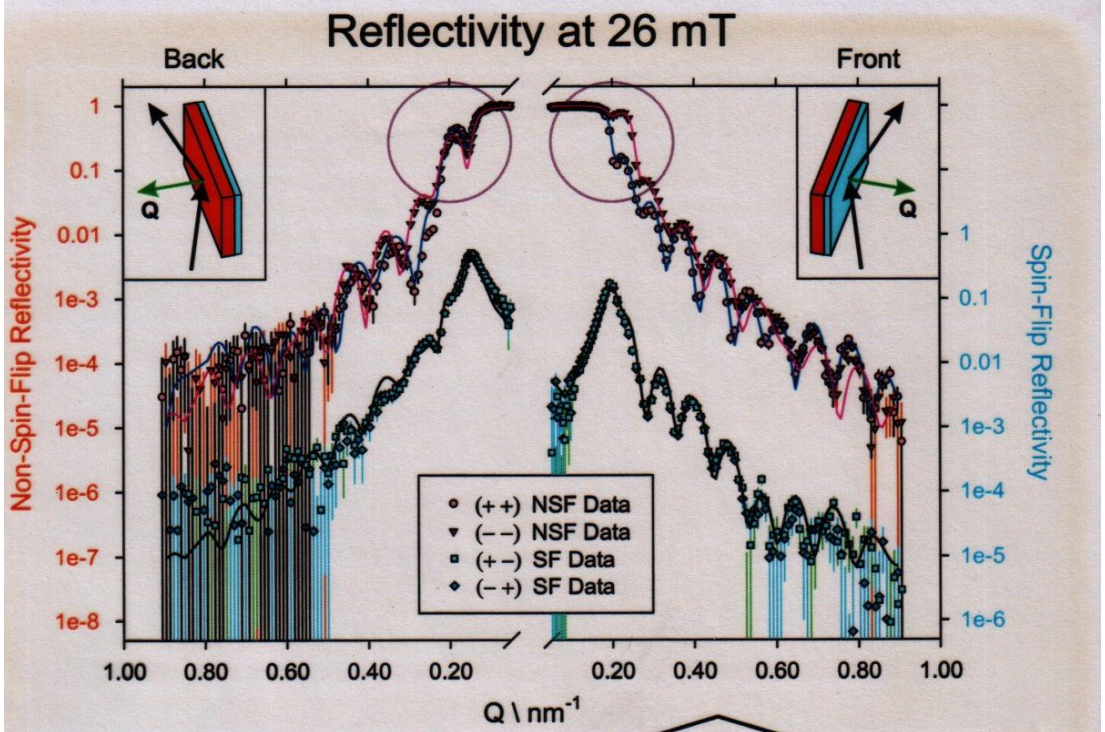

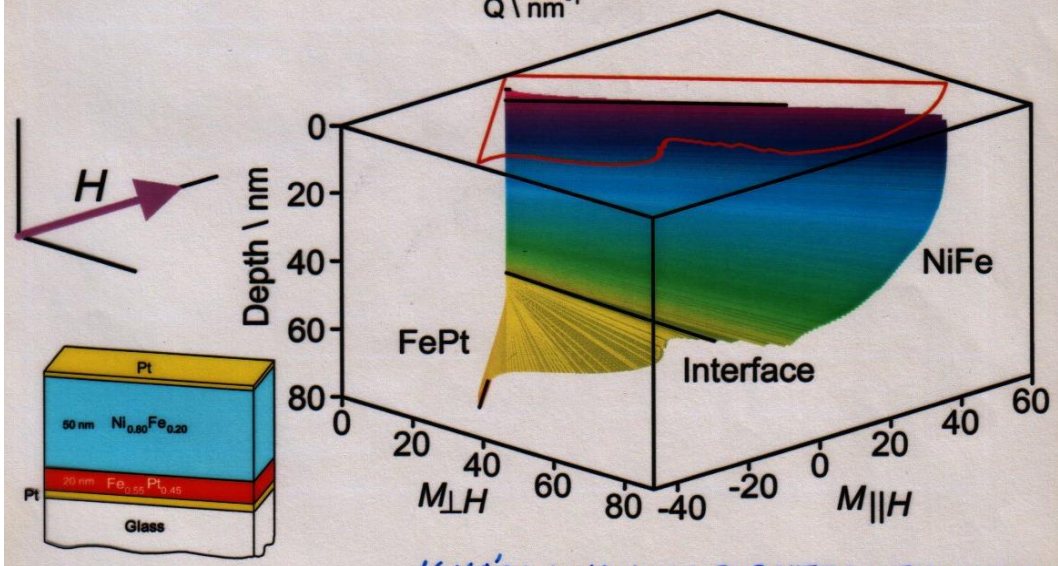

Deposited using magnetron sputtering
FePt codeposited from elemental targets
NiFe deposited from alloy target

K. V. O'DONOVAN, J. A. BORCHERS, C. F. MAJKRZAK, O. HELLWIG, E. E. FULLERTON

Magnetic Multilayers and Thin Films

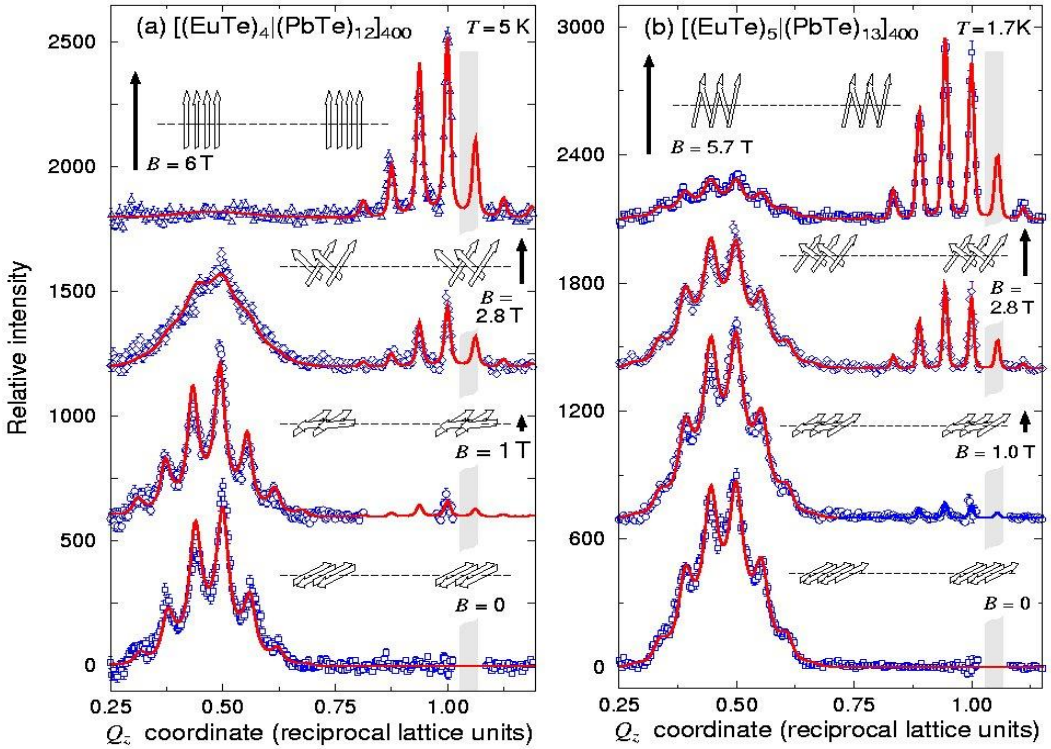

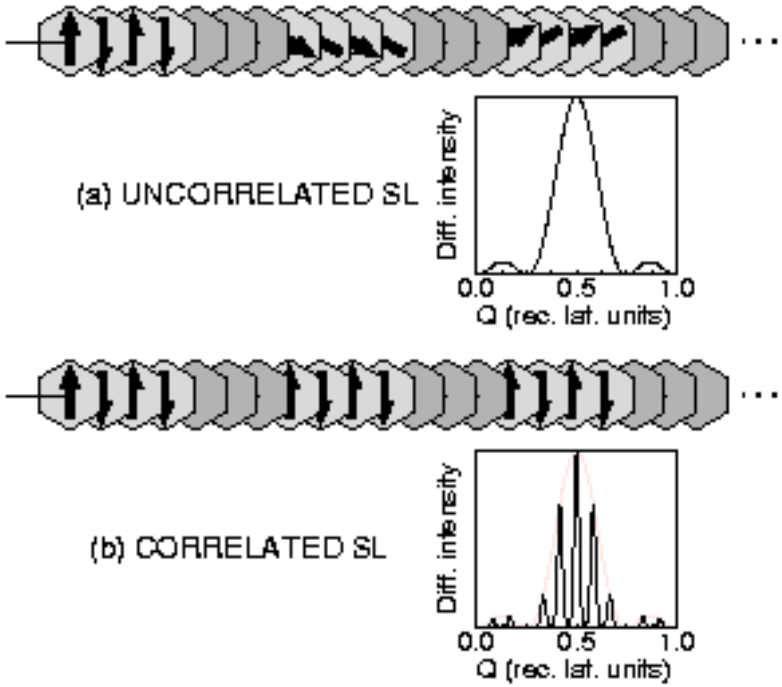

Polarized neutron reflection data on magnetic semiconductor superlattices by Henryk Kepa et al..

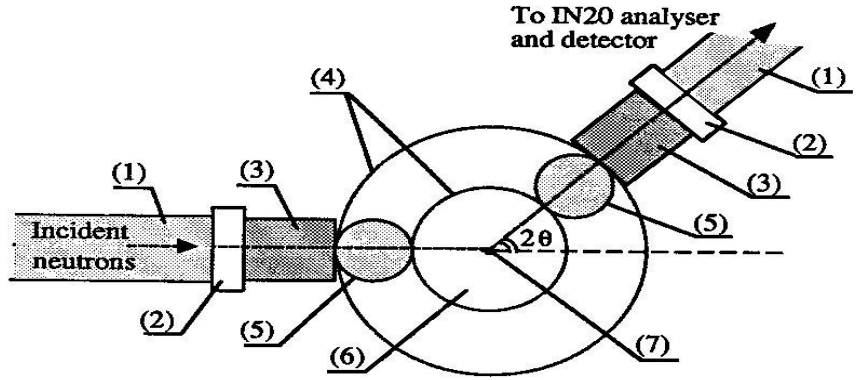

Fig. 3.2 Schematic horizontal cross-section of CRYOPAD showing: (1) axial guide field; (2) non-magnetic rotation unit; (3) nutation guide field (4) concentric test-tube shaped Meissner shields; (5) vertical super-conducting solenoids producing a precession field of up to 100 Oe; (6) zero field sample chamber containing a variable temperature insert which allows sample temperatures in the range 1.5 K to 300 K; (7) Sample position. Note that the contents of the cryostat tail are enlarged in the diagram for clarity - actual sizes are: inner Meissner screen diameter = 40 mm, precession solenoid diameter 13 mm, nutation guide diameter approximately 100 mm.

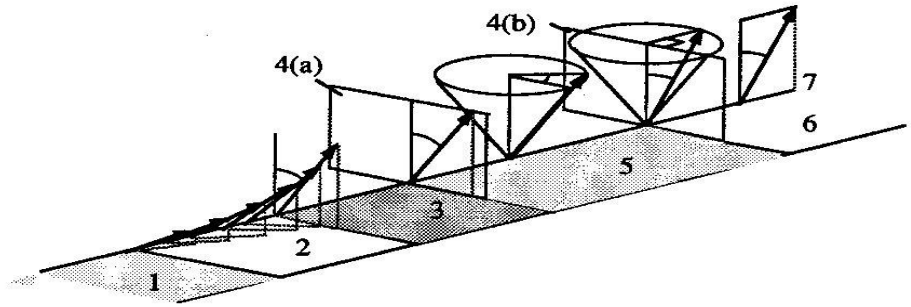

Fig. 3.4 Diagram showing what happens to the polarization of the incident neutrons during their passage through the different field regions of the instrument towards the sample position. In region (1), incident neutrons are polarized axially. In region (2), fields of (1) and (3) overlap, polarization rotates adiabatically to the direction of nutation field. As neutrons pass through the Meissner shield (4) the polarization is unchanged, then, in region (5), the polarization precesses around the vertical field axis. On reaching the second Meissner screen, neutron polarization has precessed by a total angle ϕ, and once in zero-field (6), polarization is preserved up to sample position (7). Thus by choosing the angle of the nutation guide field and the current through the precession field, one can have any required direction of incident polarization at the sample position.

Zero-field neutron polarimetry (figure from thesis of Valerie Nunez)

P.J.Brown, V.Nunez, F.Tasset, J.B.Forsyth and P.Radhakrishna
J.Phys.:Condens.Matter **2** (1990) 9409
Determination of the magnetic structure of Mn_3Sn using generalized neutron polarization analysis

V.Nunez, P.J.Brown, J.B.Forsyth and F.Tasset
Physica B **174** (1991) 60
Zero-field neutron polarimetry

P.J.Brown, T.Chattopadhyay, J.B.Forsyth, V.Nunez and F.Tasset
J.Phys.:Condens. Matter **3** (1991)
Antiferromagnetism in CuO studied by neutron polarimetry

V.Nunez, P.J.Brown, T.Chattopadhyay, J.B.Forsyth and F.Tasset
Physica B - in print
Magnetic structure determination using zero-field neutron polarimetry

V.Nunez, R.Trump, P.J.Brown, T.Chattopadhyay, M.Loewenhaupt and F.Tasset
J.Phys.:Condens. Matter - submitted
Antiferromagnetism of the Kondo lattice compound $CeCu_2$ studied by neutron polarimetry

P.J.Brown, V.Nunez, F.Tasset and J.B.Forsyth
Acta Cryst. - submitted
Extinction in mixed magnetic and nuclear reflections. A study of the magnetic structure of $TbAlO_3$ using zero-field neutron polarimetry and integrated intensity measurements

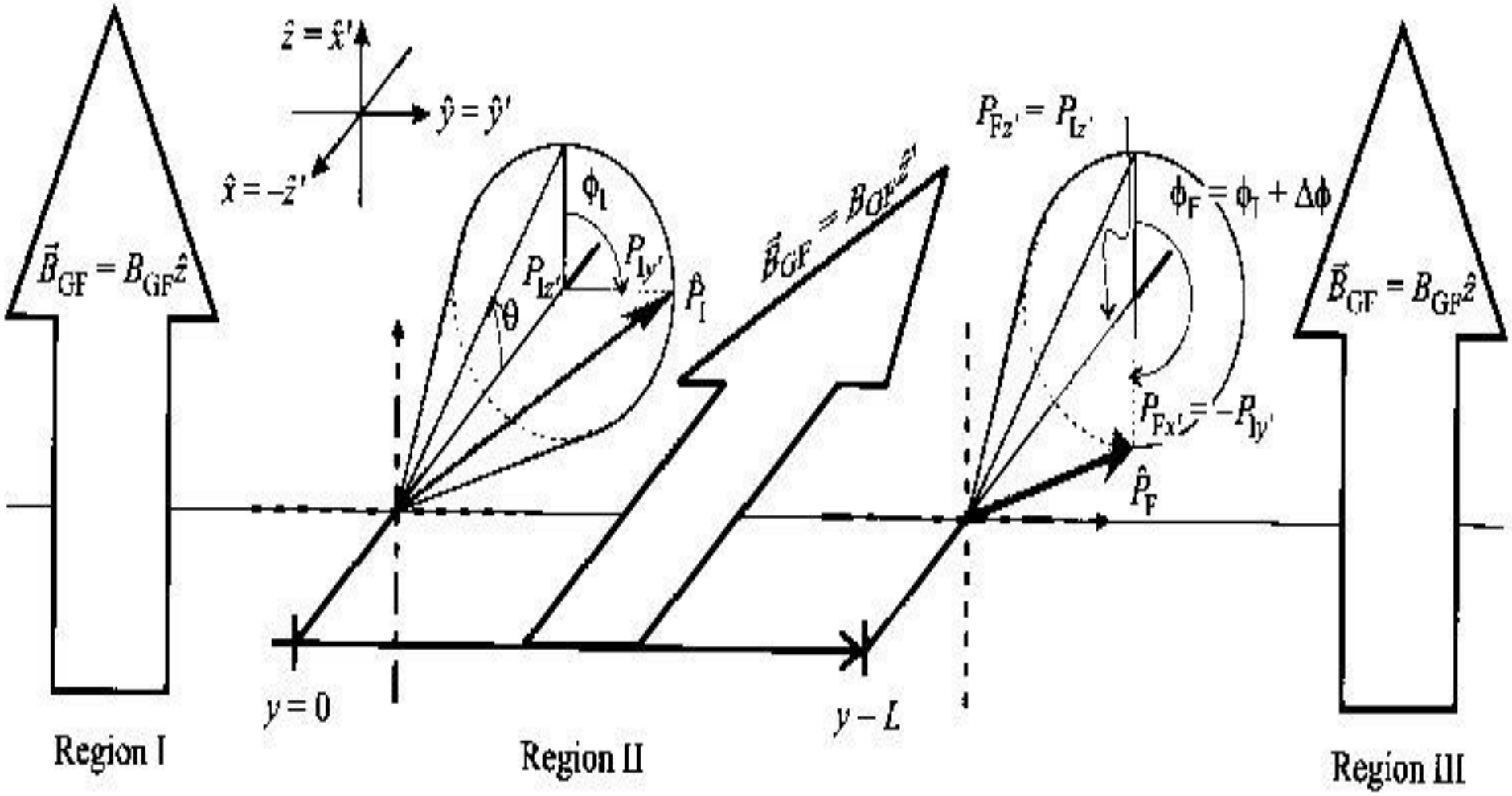

Fig. 11. Magnetic guide field configuration along the neutron trajectory (y axis) similar to that shown in Figure 10, but for a more general initial neutron polarization at $y = 0$. Note that as the neutron polarization precesses through Region II, its projection along the field direction (z' axis) remains constant. The component along the y' axis, however, is rotated to point along the $-x'$ axis at $y = L$.

$$\Psi(\vec{r}, s) = C_+ \begin{pmatrix} 1 \\ 0 \end{pmatrix} \Psi_+(\vec{r}) + C_- \begin{pmatrix} 0 \\ 1 \end{pmatrix} \Psi_-(\vec{r})$$

$$|C_\pm|^2 = C_\pm^* C_\pm$$

$$n_\pm = \sqrt{1 - 4\pi(\rho_N \pm \rho_M)/k_0^2}$$

$$\begin{pmatrix} C_+^* & C_-^* \end{pmatrix} \begin{pmatrix} C_+ \\ C_- \end{pmatrix} = |C_+|^2 + |C_-|^2 = 1$$

$$P_x = 2\,\mathrm{Re}(C_+^* C_-) = \sin\theta \cos\phi$$

$$P_y = 2\,\mathrm{Im}(C_+^* C_-) = \sin\theta \sin\phi$$

$$P_z = |C_+|^2 - |C_-|^2 = \cos\theta$$

e.g., precessing about $\hat{z}$-axis while propagating along $\hat{y}$-axis:

$$P_{Y_F}(y) = \sin[(n_- - n_+) k_0 y]$$

(for $P_{Y_I}(y=0) = 0$)

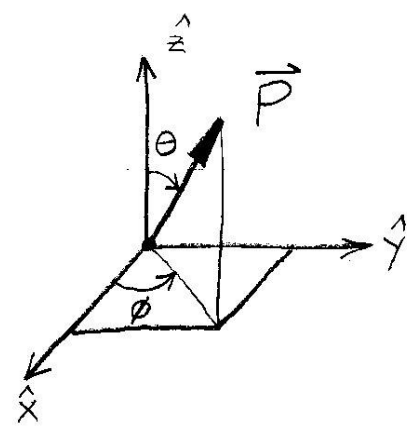

Vertical Sample Neutron Reflectometer @ Guide NG-1

The VREFL reflectometer uses a vertically focusing pyrolytic graphite monochromator to intercept the full height (15 cm) and width (6 cm) of the beam in the NG-1 guide and focuses it down to ~ 3 cm at the sample. Adjustable slits after the monochromator and in front of the sample, 1.5 m away, define the beam width and collimation. Highly efficient (polarization > 98 %, and transmission of one spin state ~ 80 %) supermirror polarizers, shown in the photo below, may be inserted in the incident and reflected beams to provide full polarization analysis. Overall instrumental flipping ratios of the order of 100 are routinely achieved.

Instrument Specifications	
Wavelength, & resolution	4.75 Å, 1.5 % $\Delta\lambda/\lambda$
Q-resolution nearly constant	$\Delta Q/Q = 0.025$
Flux at sample	10^5 n/cm^2-s typically
Minimum measurable reflectivity	$< 10^{-8}$

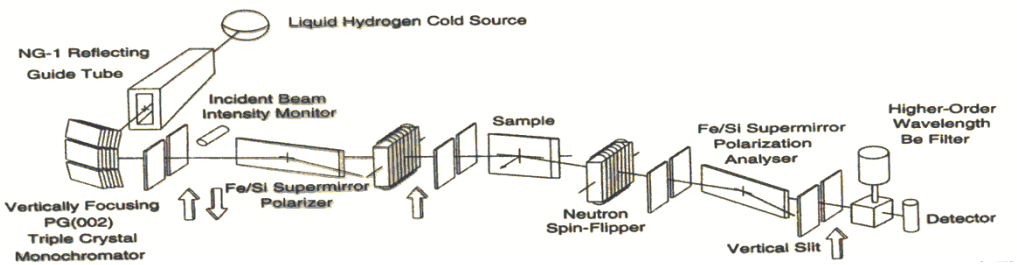

The vertical sample reflectometer configured with polarizing supermirrors before and after the sample

In situ capabilities including:

- Cryostats (50mK<T<675K)
- Magnetic fields (0 to 0.7 Telsa)
- Vacuum Furnaces 77K<T<2,073K
- Electrochemical Cells
- Liquid Cells
- Controlled Humidity Cells

Neutron spin echo labelling of angle: after work of Felcher, te Velthuis, Rekveldt, Pynn, Major and others. (Thanks to Suzanne te Velthuis for next three figures!)

α_i, α_f Resolve 2 dimensions with Slits and PSD

φ Resolve 3rd dimension with Spin Tagging

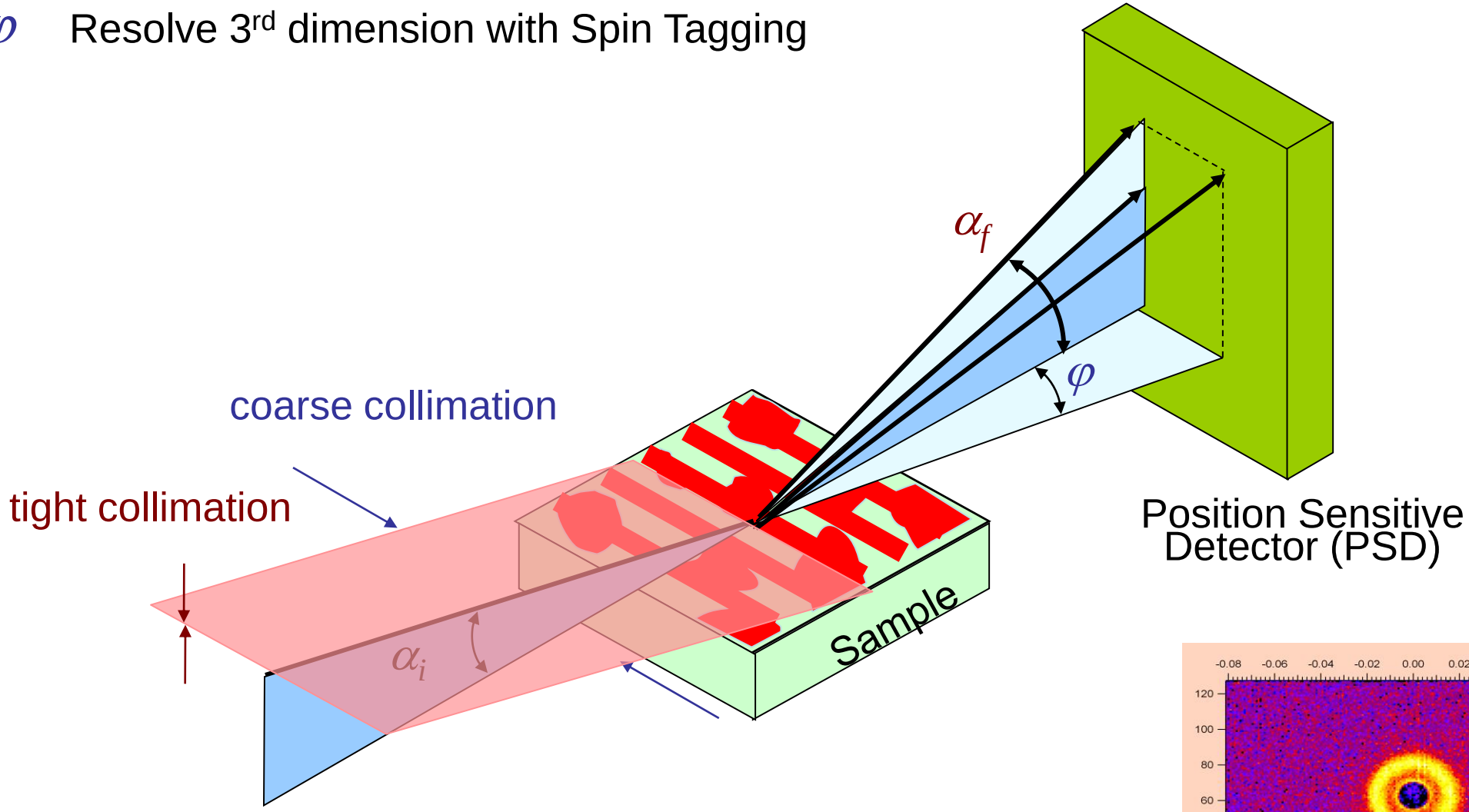

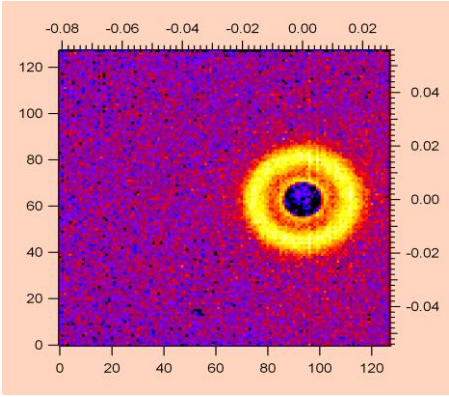

Provides 3-D analysis of surface and sub-surface feature in nanostructures

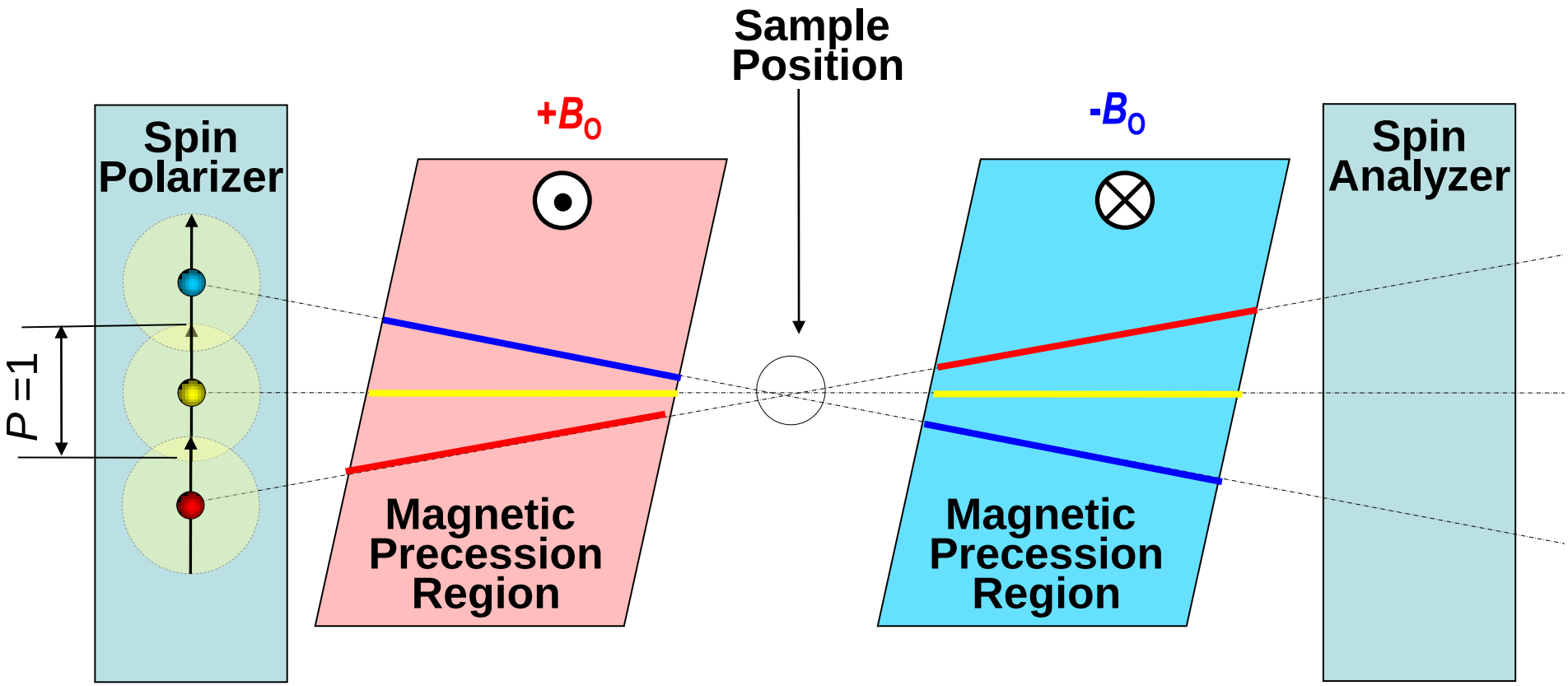

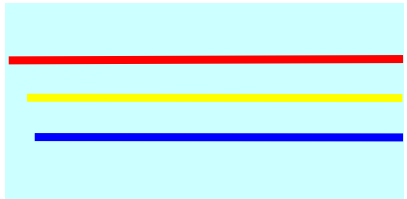

Different Path Lengths for
Different Trajectories

Encoding enables resolution of in-plane structure without prohibitive intensity loss.

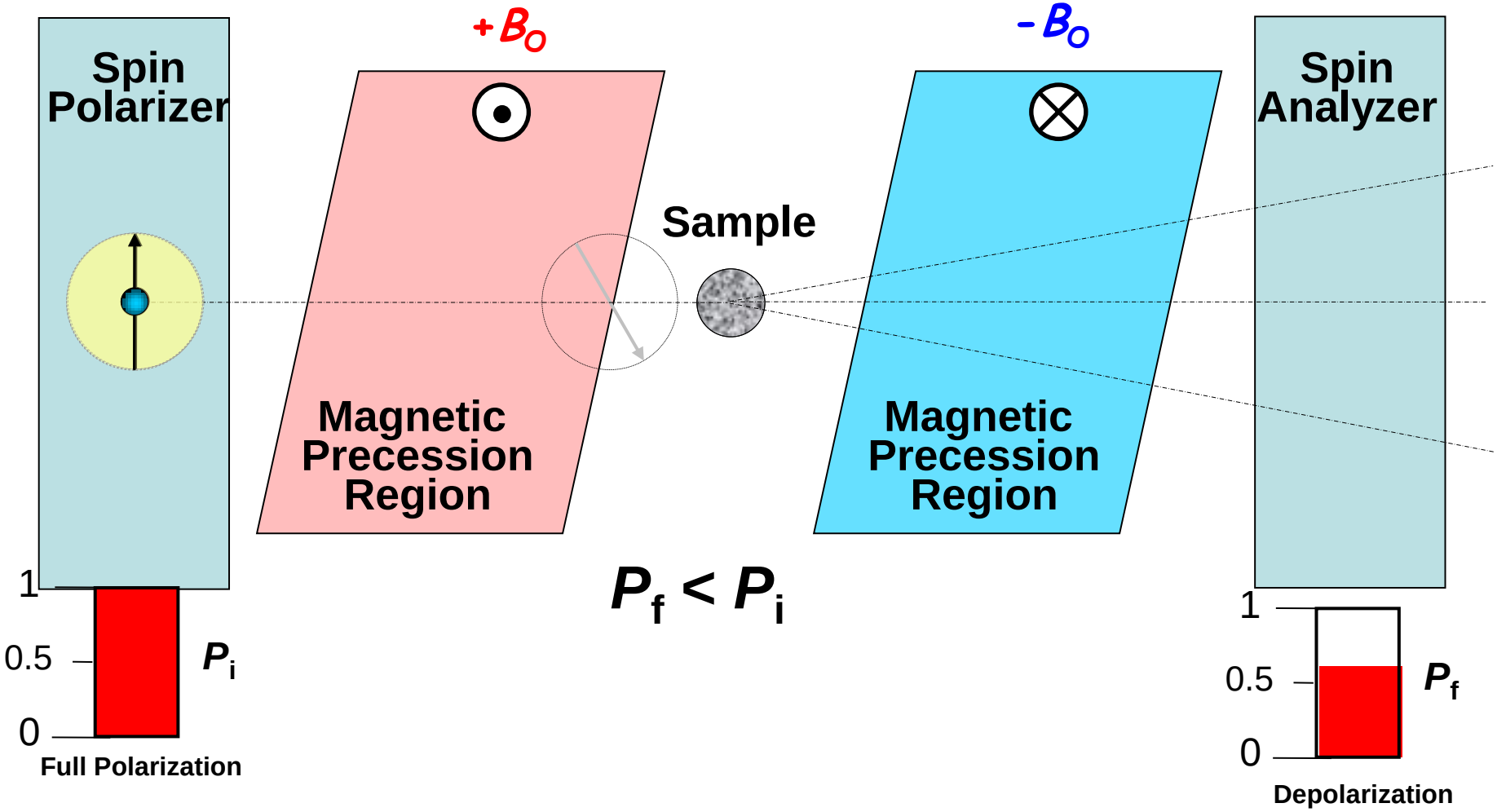

NSE LABELLING OF ANGLE : PRECESSION FIELD GEOMETRY

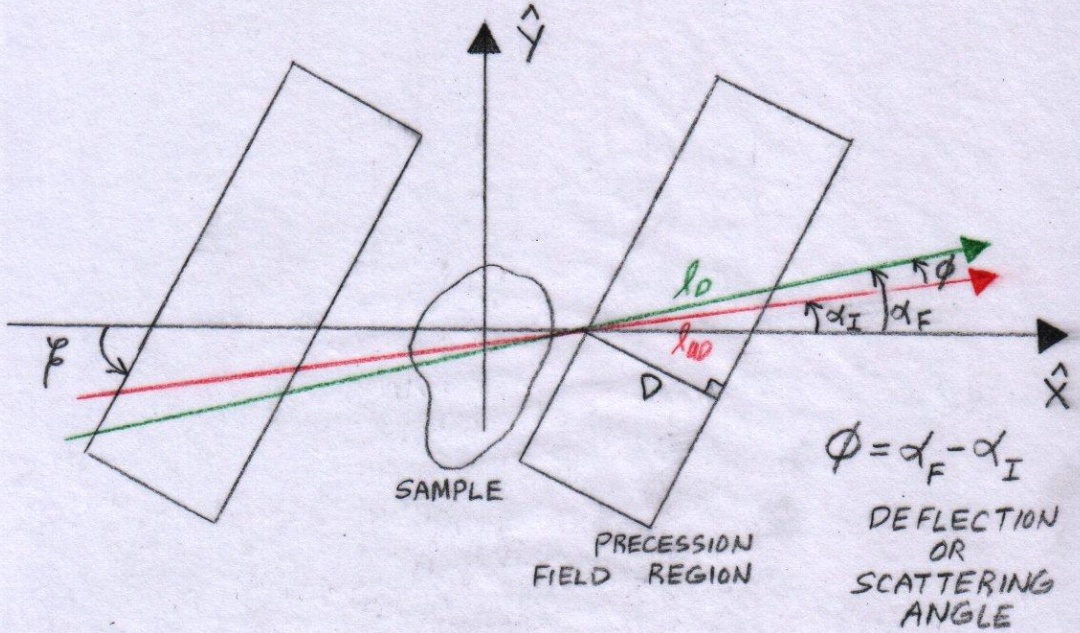

$$\phi = \alpha_F - \alpha_I$$

DEFLECTION OR SCATTERING ANGLE

$$l_D \sin(\xi - \alpha_F) = D = l_{UD} \sin(\xi - \alpha_I)$$

PATH LENGTH <u>DIFFERENCE</u> $\Delta l = l_D - l_{UD}$

$$\Delta l = D\left[\frac{1}{\sin(\xi - \alpha_F)} - \frac{1}{\sin(\xi - \alpha_I)}\right]$$

AT SUFFICIENTLY SMALL ANGLES

$$\Delta l \simeq D\left[\frac{(\alpha_F - \alpha_I)}{(\xi^2 - \alpha_F \xi - \alpha_I \xi + \alpha_F \alpha_I)}\right]$$

J. Major et al., Physica B 336 (2003) 8-15

$$Q_y \simeq k(\alpha_F - \alpha_I) \equiv k\phi$$

$$|r_{BA}(Q_y)|^2 \propto \left| \int \rho(y) e^{iQ_y y} dy \right|^2$$

$$P_x(\delta^{SE}) = \int |r(\phi)|^2 \cos(k\phi\delta^{SE}) d\phi$$

WHERE $\underbrace{\delta^{SE}}_{\text{SPIN ECHO "LENGTH"}} = \left[\underbrace{\left(\frac{m_n \gamma_n \lambda^2}{2\pi h} \right)}_{\text{CONSTANT}} \left(\frac{B\,D}{\sin\xi} \frac{\cos\xi}{\sin\xi} \right) \right]$

PRECESSION FIELD TILT ANGLE

DIFFRACTION FROM GRATING STRUCTURE ALONG Y-DIRECTION (IN PLANE)

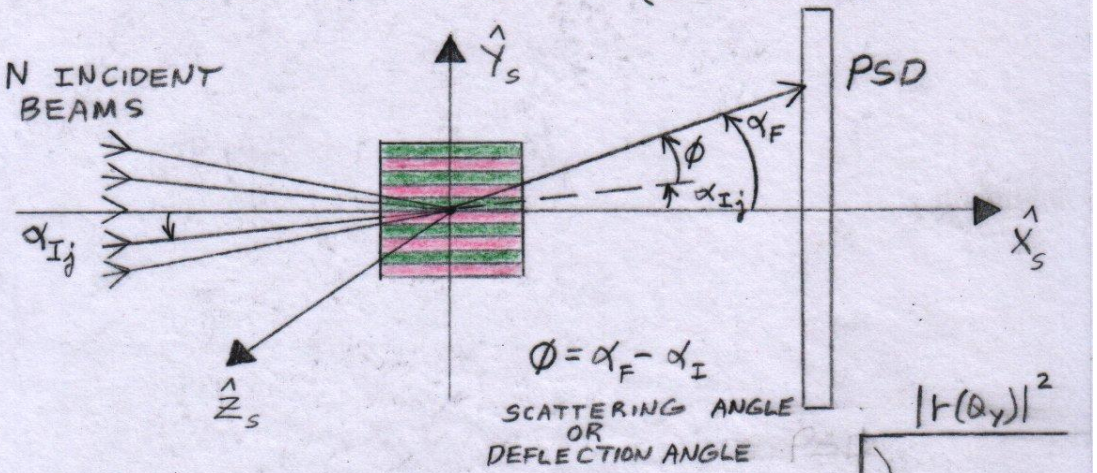

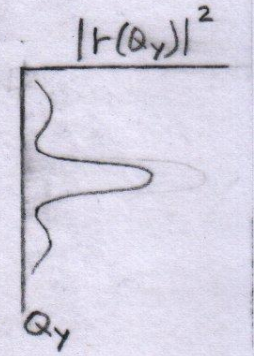

SOLVE SET OF SIMULTANEOUS EQUATIONS FOR $|r|^2$

$$\underbrace{S(\delta_i)}_{\substack{S_1 \\ S_2 \\ \vdots \\ S_N}} = \sum_{j=1}^{N} I_0 \underbrace{M(\delta_i, \alpha_{I_j}, \alpha_F)}_{\text{MODULATION FUNCTION}} \left| r(\alpha_F, \alpha_{I_j}) \right|^2$$

(δ_i = MODULATION PARAMETER)

$|r|^2 \equiv \dfrac{\text{REFLECTED INTENSITY}}{\text{INCIDENT INTENSITY}}$

e.g., $$M = \frac{I_\pm}{I_0} = \left[\frac{1 \pm \cos\beta}{2}\right]$$

OR

$$M = P_x = \frac{I_+ - I_-}{I_+ + I_-} = \cos\beta$$

WHERE β = CONSTANT $B\,\Delta\ell$

AND $$\Delta\ell = \left[\frac{D(\alpha_F - \alpha_I)}{(\xi^2 - \alpha_F \xi - \alpha_I \xi + \alpha_F \alpha_I)}\right]$$

ξ = "TILT" ANGLE OF RECTANGULAR PRECESSION FIELD REGION

> Sum over reflected intensities, contributed by each corresponding incident beam, at a given detector position (angle) and repeat for all other available detector positions (data collected simultaneously).

> Depending on the type of scattering system, it may be possible to add reflected intensities at all detector positions together if terms can be regrouped and collected in such a way as to correspond to the same effective scattering angle or value of *Qy*.

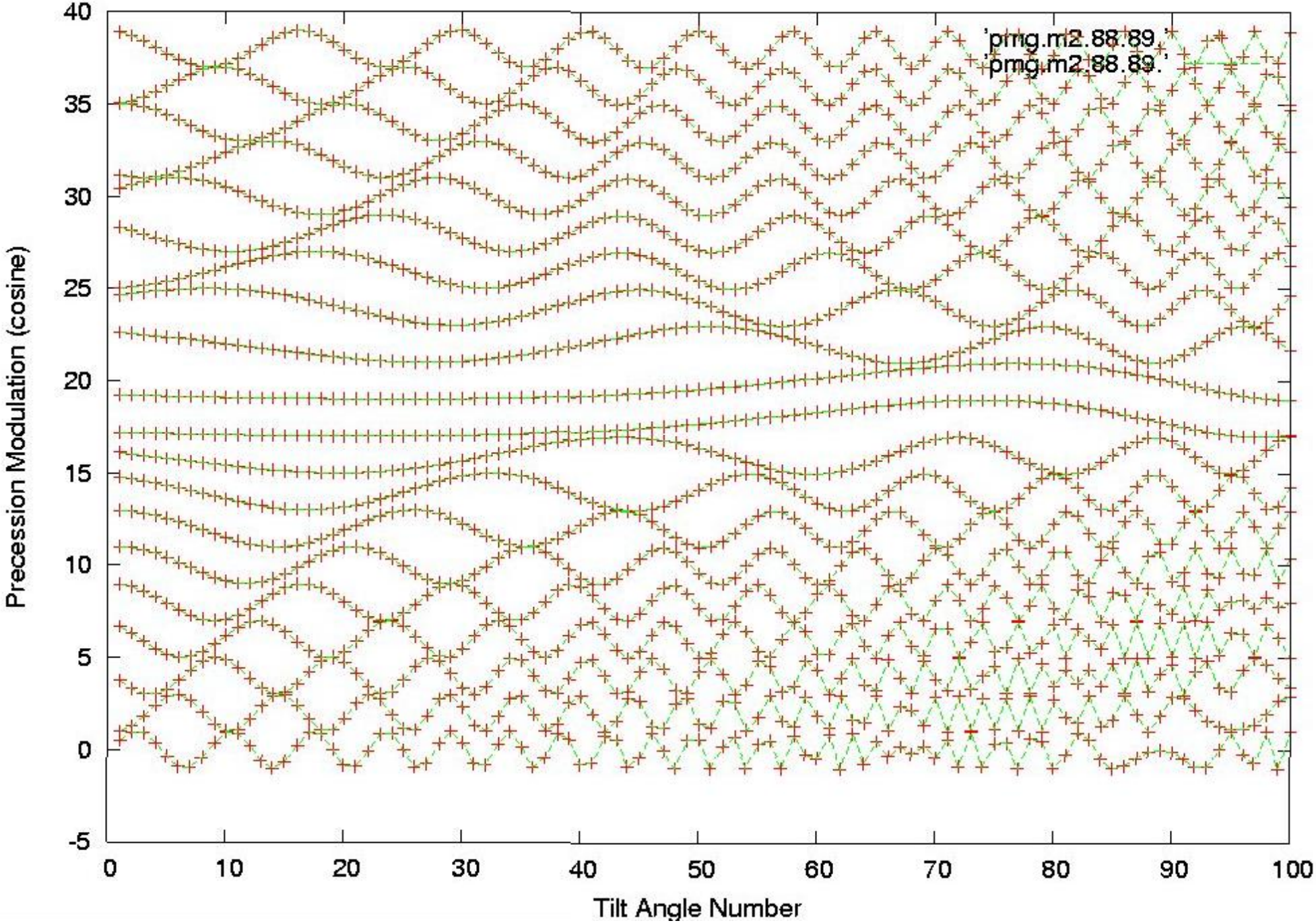
'pmg.m2.88.89.'
'pmg.m2.88.89.'
Precession Modulation (cosine)
Tilt Angle Number
40
35
30
25
20
15
10
5
0
-5
0
10
20
30
40
50
60
70
80
90
100

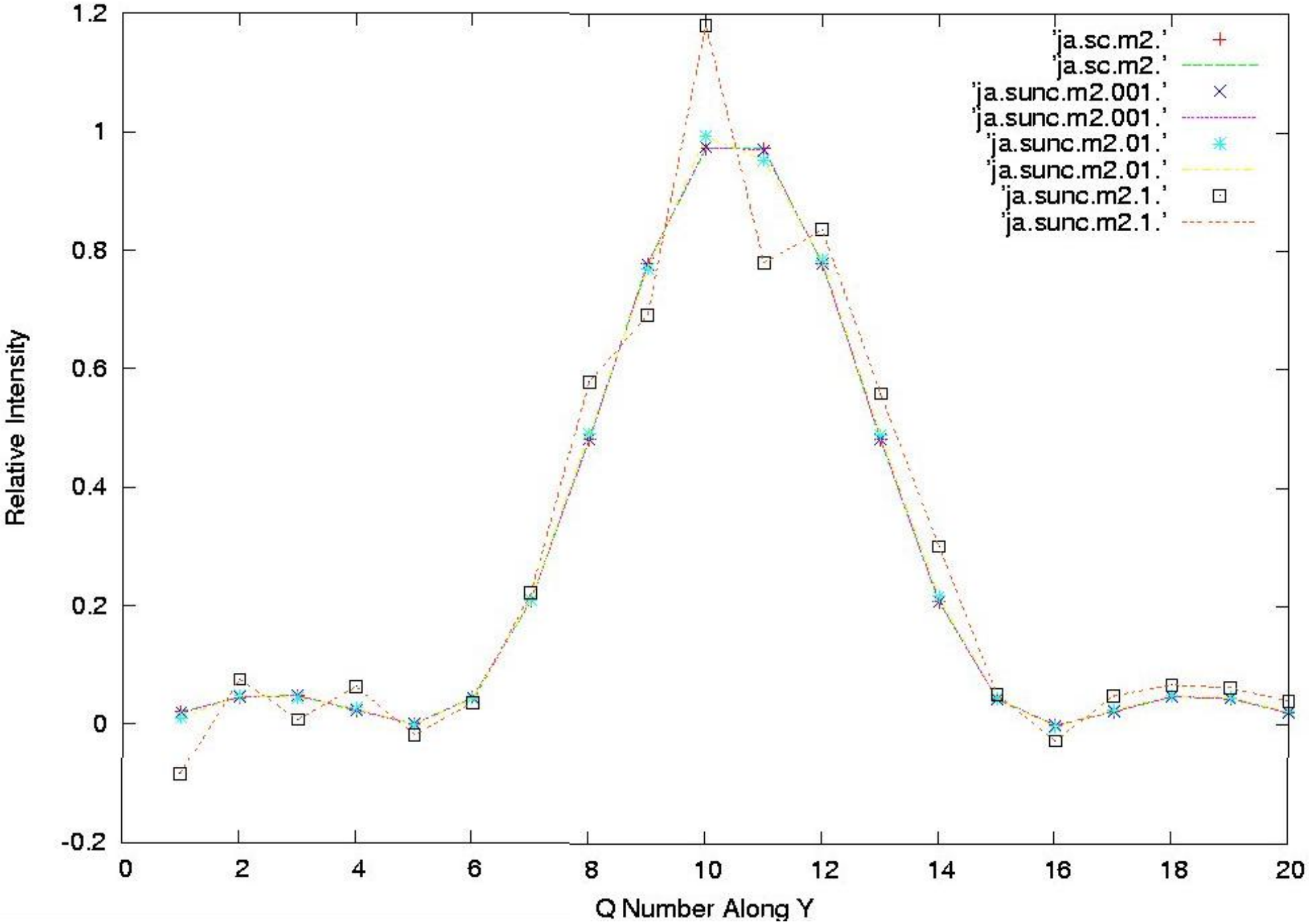
'ja.sc.m2.'
'ja.sc.m2.'
'ja.sunc.m2.001.'
'ja.sunc.m2.001.'
'ja.sunc.m2.01.'
'ja.sunc.m2.01.'
'ja.sunc.m2.1.'
'ja.sunc.m2.1.'
Relative Intensity
Q Number Along Y
1.2
1
0.8
0.6
0.4
0.2
0
-0.2
0
2
4
6
8
10
12
14
16
18
20

Compact magnetic films replace precession coils.

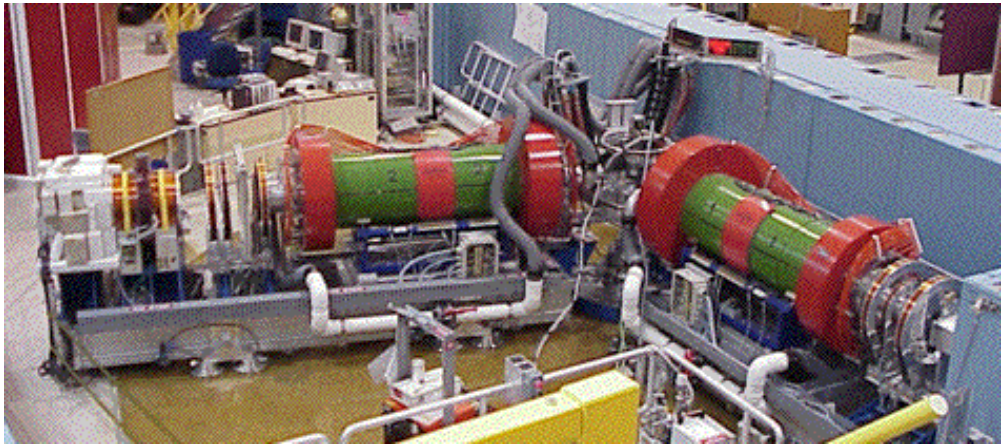

Spin Echo Spectrometer
on NG5 at the NCNR

Spin Tagging Demonstration[1]
on EVA at the ILL, France

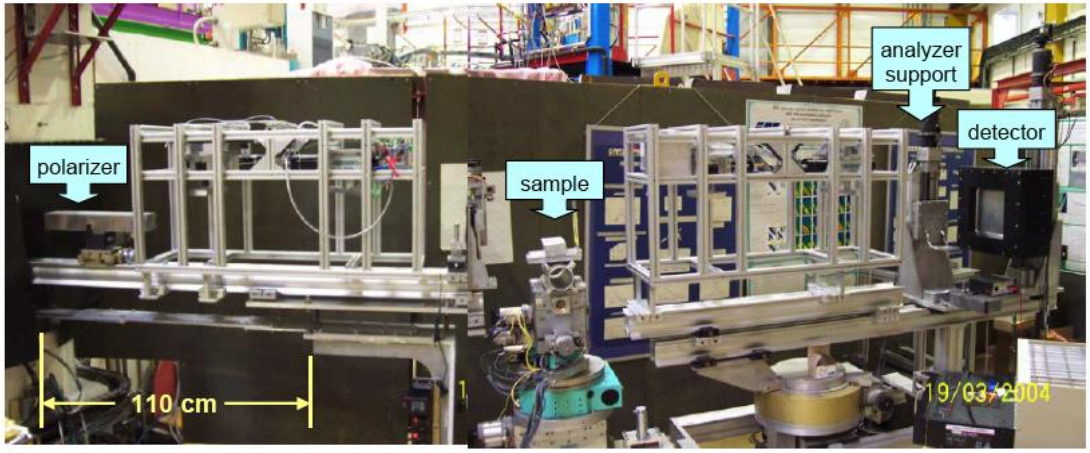

[1]J. Major, H. Dosch, G.P. Felcher, *et al*., Physica B (2003).
Also, M. Th. Rekveldt, *et al.,* Rev. Sci. Instr. (2005).
And R. Pynn, M.R. Fitzsimmons, *et al*., Rev. Sci. Instr. (2005).

“Polarized Neutron Reflectometry”, C.F.Majkrzak, K.V.O'Donovan, and N.F.Berk, Chapter 9 in *Neutron Scattering from Magnetic Materials*, Edited by T.Chatterji, (Elsevier, Amsterdam, 2006) p.397-471.

Polarized Neutrons, W. Gavin Williams, (Clarendon Press, Oxford, 1988)